TECHNISCHE UNIVERSITÄT DRESDEN

Fakultät Umweltwissenschaften Institut für Hydrologie und Meteorologie

ON THE DERIVATION OF SPATIALLY HIGHLY RESOLVED PRECIPITATION CLIMATOLOGIES UNDER CONSIDERATION OF RADAR-DERIVED PRECIPITATION RATES

Cumulative Dissertation to achieve the academic degree of
Doctor rerum naturalium (Dr. rer. nat.)

submitted by

Dipl.-Hydrol. Rico Sascha Kronenberg

born on 29 October 1985 in Räckelwitz, Germany

Mat.-Nr.: 3221195

Referee:
Prof. Dr. Christian Bernhofer

Second Referee:
Prof. Dr. Clemens Simmer

Third Referee:
Prof. Dr. Lars Bernard

Submitted on 15. Oktober 2014

ERKLÄRUNG DES PROMOVENDEN

Die Übereinstimmung dieses Exemplars mit dem Original der Dissertation zum Thema:

"On the derivation of spatially highly resolved precipitation climatologies under consideration of radar-derived precipitation rates"

wird hiermit bestätigt.

Dresden, 20. Juli 2015

Rico Kronenberg

ABSTRACT

In this cumulative dissertation, different features and methods are presented to assess and process multi-sensor derived radar data for climatological analysis. The overall objectives were to appraise the limitations of an hourly radar-based quantitative precipitation estimate (QPE) product and to develop and apply reasonable approaches to process these data. Hence the spatial and temporal limitations of radar-derived precipitation rates are discussed in the context of climatological applications, and two types of climatologies are obtained, first a climatology of daily precipitation fields and second a long term precipitation climatology. These relate to questions concerning the methodologies rather than climatological significance or assessment of precipitation and its role in the water balance. Current radar data availability limits such a hydro-climatic analysis.

The thesis consists of three peer-reviewed publications. All investigations in this thesis are based on the RADOLAN rw-product of the German Weather Service (DWD) for an extended study region including the Free State of Saxony, Germany, for the period from April 2004 to November 2011.

The first publication is dedicated to the classification of daily precipitation fields by unsupervised neural networks. In the presented work, the quality of the radar-derived precipitation rates is analysed by a temporal comparison between recording and non-recording gauges and the corresponding pixels of the RADOLAN rw-product on hourly and daily bases. The analysis shows that a temporal aggregation of the original product should be limited to a temporal scale up to 24 h because of the processing algorithms and the reappearance of previously suppressed errors. Nevertheless, an unsupervised neural network was successfully used for the classification of daily patterns. The derived daily precipitation classes and corresponding precipitation patterns could be assigned to properties of the associated weather patterns and seasonal dependencies. Hence, it could be shown that the classified patterns not only occurred by chance but by statistically proven properties of the atmosphere and of the season.

The second publication is primarily concerned with two tasks: first, the pixel-wise fitting of mixture distributions on the bases of the obtained patterns from the first publication, and second, the analysis of spatial consistency of the radar-derived precipitation data set. The fitted parametric distribution functions were analysed in terms of Akaike's information criterion and the Kolmogorov-Smirnov test. These benchmarks showed, that the performances are best for mixture distributions derived by an initial classification by an unsupervised neural network and cluster analysis, and by gamma distributions. These results underline the significance of the derived precipitation classes obtained in the first publication. Furthermore, the Kolmogorov-Smirnov test indicates that independent of the distribution function, the radar-derived daily precipitation rates under the assumption of the deployed parametric distribution function has the best or most natural order of precipitation rates at spatial scales from 2 to 4 km for daily precipitation fields. Thus, it is recommended to use the original radar product at these scales rather than at 1 km resolution for daily precipitation sums.

In the last publication, the focus shifts from daily to long-term precipitation climatology. The work introduces a rapid and simple approach for processing radar-derived precipitation rates for long-term climatologies. The method could successfully be applied to the radar-derived precipitation rates by excluding or correcting the errors that reappear due to temporal aggregation. Despite the fact that the approach is empirical, the introduced parameters could almost be objectively derived by means of simulation and optimisation. This could be achieved by utilising the reasonable relationship between elevation and precipitation rates for longer periods. Finally, the obtained results are compared to two independently derived precipitation data sets. The comparison shows good agreement of the precipitation fields and illustrates a reasonable application of the introduced procedure. The presented results support the application of the approach for precipitation aggregates of, at least, annual or longer periods.

However the derivation of climatologies led to satisfactory results at the respective temporal scales, though the influence of radar-specific errors can only be minimized to a certain degree. Further studies have to prove if an application independent processing of radar-derived precipitation rates leads to higher qualities and validities of the derived data in time and space.

ZUSAMMENFASSUNG

In dieser kumulativen Dissertation werden verschiedene Eigenschaften und Methoden vorgestellt, welche der Bewertung und Prozessierung von Multi-Sensor-Radardaten für klimatologische Anwendungen dienen. Die übergeordneten Zielstellungen sind zum einen die Beurteilung der Grenzen von stündlichen Quantitativen Niederschlagsraten (QPE) und zum anderen die Entwicklung und Anwendung von geeigneten Verfahren, um diese Daten zu prozessieren. Aus diesem Grund werden die räumlichen und zeitlichen Grenzen von radarabgeleiteten Niederschlägen vor dem Hintergrund der klimatologischen Anwendung diskutiert. Dafür werden zwei Arten von Klimatologien abgeleitet, eine Klimatologie täglicher Niederschlagsfelder und ein Langzeitklimatologie. Diese sind verbunden mit Fragen, welche sich eher mit der Methodik befassen, als mit der klimatologischen Bedeutung oder der langzeitlichen Beurteilung des Niederschlags und seiner Rolle im Wasserhaushalt. Denn eine zu kurze Radardatenverfügbarkeit steht derzeit einer belastbaren klimatologischen Auswertung im Wege.
Diese Dissertation fasst die Ergebnisse dreier fachbegutachteter Veröffentlichungen zusammen. Alle Untersuchungen dieser Arbeit erfolgen anhand des RADOLAN rw-Produktes des Deutschen Wetter Dienstes (DWD) für ein erweitertes Datengebiet um den Freistaat Sachsen, Deutschland im Zeitraum April 2004 bis November 2011.
Die erste Veröffentlichung befasst sich mit der Klassifikation von täglichen Niederschlagsfeldern durch unüberwachte Neuronale Netze. In dieser Publikation wird die Qualität von radarabgeleiteten Niederschlagsraten durch den Vergleich zwischen automatischen, nicht-automatischen Regenschreibern und den zugehörigen Pixel des RADOLAN rw-Produktes in stündlicher und täglicher Auflösung bewertet. Diese Analyse zeigt, dass die zeitliche Aggregierung des originalen Datensatzes auf maximal Tageswerte beschränkt werden sollte. Dies wird begründet mit den Prozessierungsschritten und dem Wiederauftreten von ehemals unterdrückten Fehlern im Komposit. Dennoch konnte ein unüberwachtes neuronales Netzwerk erfolgreich angewendet werden, um tägliche Muster zu klassifizieren. Die resultierenden täglichen Niederschlagsklassen und die zugehörigen Niederschlagsmuster wurden mit Eigenschaften der Großwetterlage und jahreszeitlichen Abhängigkeiten verbunden. So konnte gezeigt werden, dass die klassifizierten Muster nicht zufällig, sondern unter Berücksichtigung der atmosphärischen Eigenschaften und der Jahreszeit, gefunden wurden.
Die zweite Publikation befasst sich hauptsächlich mit zwei Aufgaben; (i) der pixelweisen Anpassung von Mischverteilungen auf Grundlage der in der ersten Veröffentlichung abgeleiteten Muster und (ii) der Analyse der räumlichen Konsistenz der Niederschlagsdaten. Die angepassten parametrischen Verteilungsfunktionen wurden mittels des Akaikes-Informationskriteriums und dem Kolomogorov-Smirnov Test analysiert. Diese Bewertungskriterien zeigen im Vergleich, dass die beste Anpassungsgüte durch Mischverteilungen und einfache Gammaverteilungen erzielt werden konnte. Die Mischverteilungen wurden dabei durch die Klassifikationen von Niederschlagsmustern mittels unüberwachten Neuronalem Netz oder Clusteranalyse initialisiert. Die Ergebnisse untermauern die Signifikanz der abgeleiteten Niederschlagsklassen der ersten Publikation. Außerdem zeigen die Ergebnisse des Kolmogorov-Smirnov Tests an, dass unabhängig der gewählten Verteilungsfunktion, die radarabgeleiteten Niederschlagsraten unter der Annahme der gewählten parametrischen Verteilungen, die beste oder natürlichste Form von Niederschlag auf räumlichen Skalen von 2 bis 4 km für tägliche Niederschlagsfelder besitzen. Deshalb scheint es besser das Originalradarprodukt in dieser Auflösung zu nutzen, als in der ursprünglichen Auflösung von 1 km für tägliche Niederschlagssummen.
In der letzten Publikation ändert sich der Fokus von täglichen zu Langzeitniederschlagsklimatologien. Die Arbeit stellt einen schnellen und einfachen Ansatz zur Prozessierung von radarabgeleiteten Niederschlagsraten für Langzeitklimatologien vor. Die Methode konnte erfolgreich auf Radarniederschläge angewendet werden. Durch das Verfahren werden Fehler entweder ausgeschlossen oder korrigiert, welche durch die zeitliche Aggregierung wieder auftreten. Abgesehen von der Tatsache, dass diese Methode empirischer Natur ist, konnten die eingeführten Parameter jedoch objektiv durch Simulation und Optimierung bestimmt werden. Dies wurde durch die Annahme einer begründeten Beziehung zwischen Geländehöhe und Niederschlagsrate für lange Zeiträume ermöglicht. Abschließend wurden die so erzielten Ergebnisse mit zwei unabhängigen Datensätzen verglichen. Dieser Vergleich weist eine gute Übereinstimmung der Niederschlagsfelder aus und

unterstützt die begründete Anwendung der vorgestellten Methode. Durch die Ergebnisse konnte somit gezeigt werden, dass das Verfahren für Niederschlagssummen von mindestens jährlicher oder geringerer zeitlicher Auflösung anwendbar ist.
Generell ist zu bemerken, dass die Ableitung von Klimatologien zufriedenstellende Ergebnisse für die jeweiligen zeitlichen Auflösungen liefern kann. Jedoch ist der Einfluss von radarspezifischen Fehlern nur bis zu einem gewissen Grad minimierbar. Zukünftige Untersuchungen werden zeigen, ob durch die Loslösung, der Prozessierung von Radardaten zur Ableitung von Niederschlagsraten, von einem bestimmten Anwendungsbezug eine höhere Qualität und eine breitere Gültigkeit der erzeugten Daten für Raum und Zeit erzielt werden kann.

CONTENTS

1 INTRODUCTION

1.1 MOTIVATION AND SCOPE

The development of radar products, or radar-based quantitative precipitation estimates (QPE), for applications in water management (Krämer and Verworn, 2005), heavy precipitation forcasts (Meetschen and Simmer, 2005), flood risk management and hydrological forecasts (Weigl and Winterrath, 2009) has reached a stage that allows for operational processing and prompt online availability of data (Becker, 2013). This evolution has been fostered by better computational resources, better measurements and more adequate data processing routines. Hence, the growing number of available national and international QPE data sets and their applications in the hydrometeorological community speak for themselves (Weigl and Winterrath, 2009; Smalley et al., 2014; Michelson and Koistinen, 2000; Walther, 2007).
Climatological aspects of radar data processing, such as precipitation patterns, long-term precipitation climatologies and extreme value analysis, were almost completely neglected during this development. More attention was paid to the development of approaches to process and assimilate real-time radar data to forecast potentially dangerous hydro-meteorological situations. Radar measurements offer high temporal and spatial density of data regarding the precipitation behaviour and have tremendous potential for climatological analysis and the assessment of the regional water cycle.
The estimation of precipitation with the help of ground-based Doppler radar technology is a complex task because the detection of precipitation fields by means of radar is based on the alternating transmitting and receiving of electromagnetic waves. The received pulsed energy enables us to draw our conclusions regarding the precipitation in the atmosphere. For example, the distance and extent of a precipitation field can be calculated through the transmission time. The backscattered portion of the transmitted energy can be converted to the reflectivity of precipitation, and by using the Doppler shift of the signal, the speed of the target can be derived.
This short and simplified summary of the fundamental principles of radar shall illustrate that precipitation measurement by radar is not a direct measurement of precipitation rates. Rather, the process of estimating the amount of precipitation is a complex procedure with several necessary steps. Early on, an additional bias correction near the end of the processing chain is applied with respect to gauge measurements. The initial investigations of the correction of bias between radar results and ground-based point measurements were conducted 28 years ago (Collier, 1986). An important figure from the study of Riedl (1986) is reproduced in Figure 1.1. The results of this study show that precipitation data from 15 regions around the weather radar Hohenpeißenberg (radar/method of areal precipitation in German 'Sammelgebietsverfahren') have an average of 95 % agreement with a standard deviation of 10 %. The agreement of the 32 single fields (radar pixel/ground-based point measurement, gauge) even reached 97 % with a standard deviation of 15 %.

Based on these results, it was concluded that better agreement between radar measurements and gauge measurements is likely to be expected as the area of averaging and the amount of temporal aggregation increase (e.g., from days to months). Unfortunately, these findings cannot be conveyed on current multi-sensor radar products. The map depicted in Figure 1.2 serves as an example. The figure is taken from Pfaff (2013) and shows the annual totals of radar-derived precipitation rates (i.e., QPEs) across Germany. It clearly shows the problems that may occur through temporal aggregation of QPEs. Residual ground clutter, shadowing effects, beam blockage and bright bands are just a few of the problems that arise. The reasons for the reappearance of those errors are manifold and differ in their origin and in the complexity of the information that is needed to cope with them. However, each of the problems in Figure 1.2 corrupts the climatological analysis and therefore must be corrected or excluded from the data set.

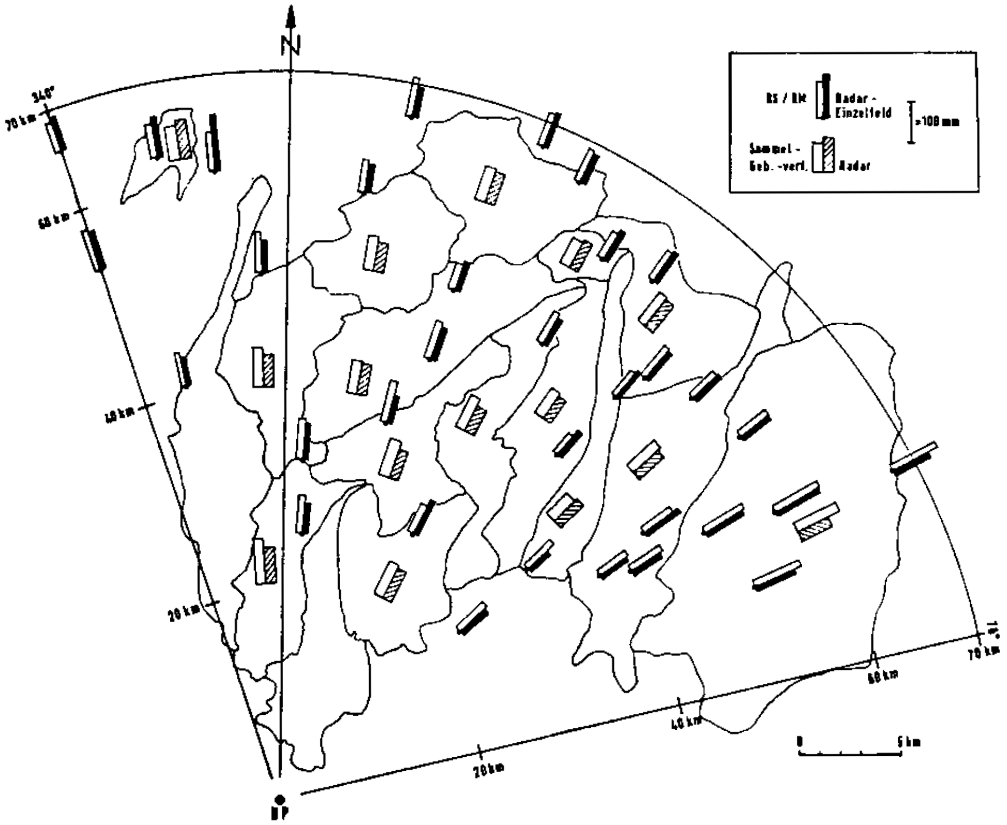

Figure 1.1: Areal total precipitation from the weather radar Hohenpeißenberg for August 1979 (without 7.,11.,18. and 26.8.) for 15 main regions that extend from 30 to 264 km. Precipitation values were calculated from radar measurements by the method of areal precipitation. Additionally, the measurements of the respective radar pixels (i.e., 1 km x 1 °) and the point measurements of the gauging stations are compared. The figure was taken from Riedl (1986).

1.1.1 Problem Formulation

This thesis is motivated by different aspects of precipitation estimation by means of radar and gauge measurement for climatological applications. The central questions address different aspects of radar climatology, from which arise the particular tasks discussed in this thesis. The central and overarching question is: How can the QPE product (i.e., the RADOLAN rw-product) of the German Weather Service (DWD) be assessed and processed for climatological analyses of precipitation fields, and what are its limitations? Therefrom result the following detailed questions:

1. Can spatially highly resolved daily precipitation fields be robustly classified into groups of similar spatial patterns?

2. What relationships exist between classes of similar daily precipitation fields, seasons and synoptic situations?

3. Do precipitation patterns improve the fitting of distribution functions on radar-derived precipitation data?

4. How do the fitted distribution functions perform over different spatial scales?

5. How can reappearing errors due to temporal aggregation of QPEs be detected and corrected for long-term climatological applications?

6. How are radar-derived long-term precipitation fields different from conventionally interpolated fields based on rain gauge data?

1.1.2 Objectives and Structure of the Thesis

This cumulative dissertation was written according to the regulations of a doctoral degree of the Faculty of Environmental Sciences at the Technische Universität Dresden.
In the latter part of this chapter, a review of precipitation estimation by means of weather radar is presented, with a focus on the description and explanation of the limitations and weaknesses of the technology. Furthermore, solutions are presented to correct known errors related to the derivation of precipitation values from radar information.
In Chapter 2, the three peer-reviewed publications can be found.
The first publication (cp. Section 2.1) presents a classification scheme to derive the climatology of daily precipitation patterns by daily radar-derived precipitation fields and the use of neural networks for classification. These pattern are linked to seasons and properties of the particular weather patterns that characterise and interpret the obtained precipitation patterns.
In the second publication (cp. Section 2.2), the derived patterns were used to estimate parameters for log-normal mixture distributions for daily precipitation rates. These distributions have the advantage of describing the probability of certain daily local precipitation rates. The resulting distributions functions were compared to other parametric distribution functions over several spatial scales. In this manner, the obtained distribution provided an indirect way of assessing the spatial quality of the data set. In addition, the field significance of the fitting quality was verified.
In the third and last manuscript (cp. Section 2.3), a rapid (i.e., in terms of computer efficiency) and simple approach is introduced and used to obtain long-term precipitation fields for climatologies from temporally aggregated radar-derived and gauge-measured precipitation rates. The annual results were compared to other independently generated precipitation data sets for the study region.
Chapter 3 presents the main findings and results from the individual publications and brings them into a common context.
Finally, in Chapter 4, an outlook of the thesis' scope is given and potential future challenges for research in the field of radar meteorology are described.
Because this is a cumulative thesis with three peer-reviewed publications, some conventions were observed regarding its structure. The symbols of all equations from Chapters 1, 3 and 4 are explained in the List of Symbols. The citations of Chapters 1, 3 and 4 can be found in the Bibliography. Equations, symbols and citations of Chapter 2 are explained in and belong to the particular publication in Chapter 2.

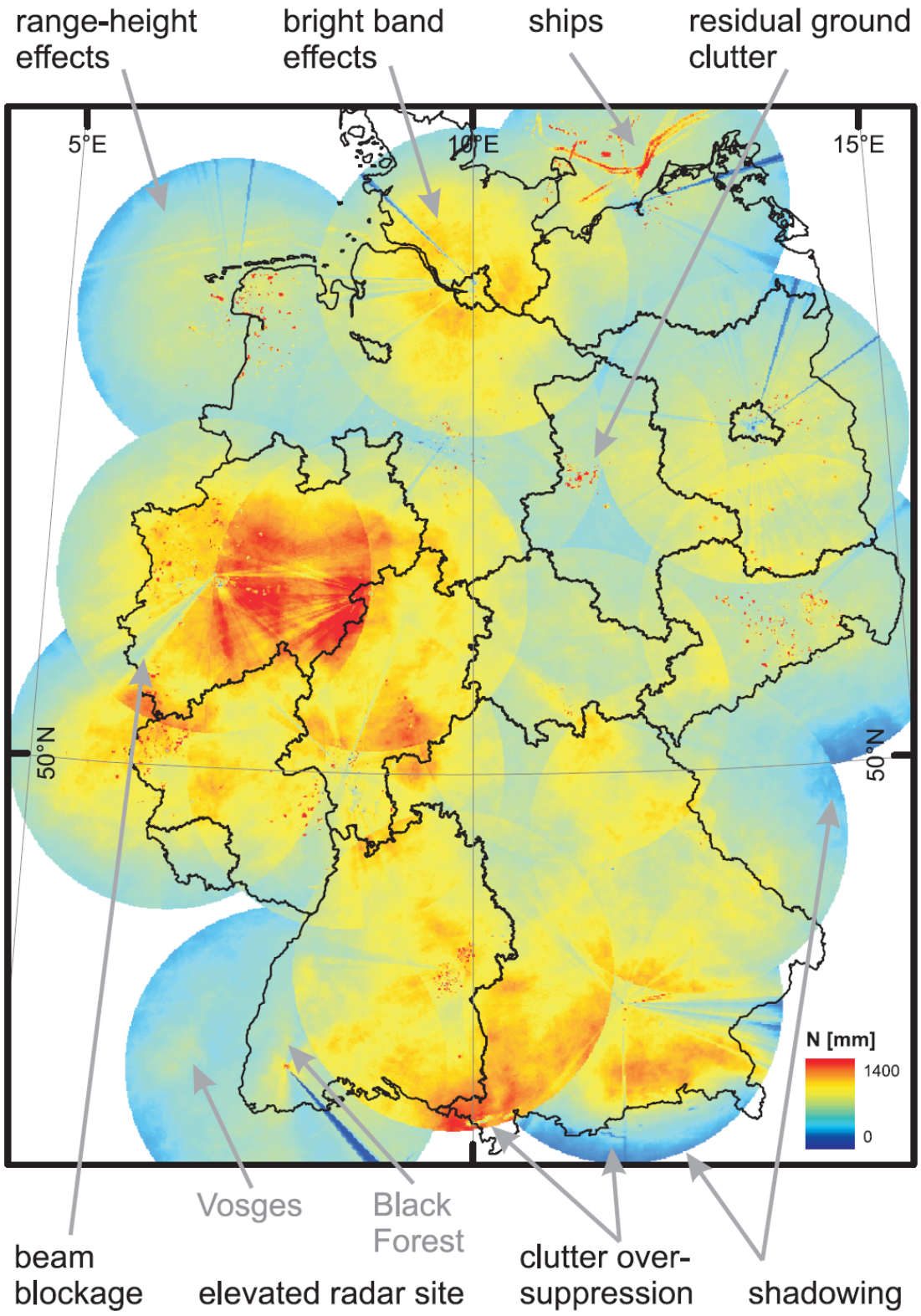

Figure 1.2: Accumulation of quality corrected precipitation estimates from radar data (German Weather Service - DWD RY-product, German composite) for the year 2009. The Figure was taken from Pfaff (2013).

1.2 PRECIPITATION AS A COMPONENT OF THE WATER BALANCE

'Nearly 80 % of all decisions are related to space.' (unknown)

This quotation, in several different forms, is often used in the field of geo-informatics to emphasise the importance of geo-referenced data (Hahmann et al., 2011). It also expresses the high significance of geographic location in human thinking and behaviour. However, what else defines, limits and characterises geographic location? From the perspective of a hydrologist, it is fast becoming clear that it is water in its manifold forms. As we know, 71 % of the Earth is covered by water (Maniak, 2010). It is joked that the most important question that bothers the hydrologist is: 'When was, is and will be where, how much water?'. In all seriousness, this question is fairly accurate in reflecting the complex set of hydrology-related questions. To answer these questions, conceptual models were developed to describe and understand the water balance (Davie, 2008). The complexity of the water balance depends on the scale considered and the accuracy claimed. The description of the water balance typically starts in textbooks from the global scale, which allows for straightforward balancing (Karamouz et al., 2013). Figure 1.3 shows the water balance at this scale with absolute figures of all components taken from Baumgartner (1996). Likewise, the water balance can be defined in its simplest form for the scale of a river basin, the regional scale, as shown in Equation 1.1 (Dyck and Peschke, 1995).

$$0 = P - E_T - Q - \Delta S \tag{1.1}$$

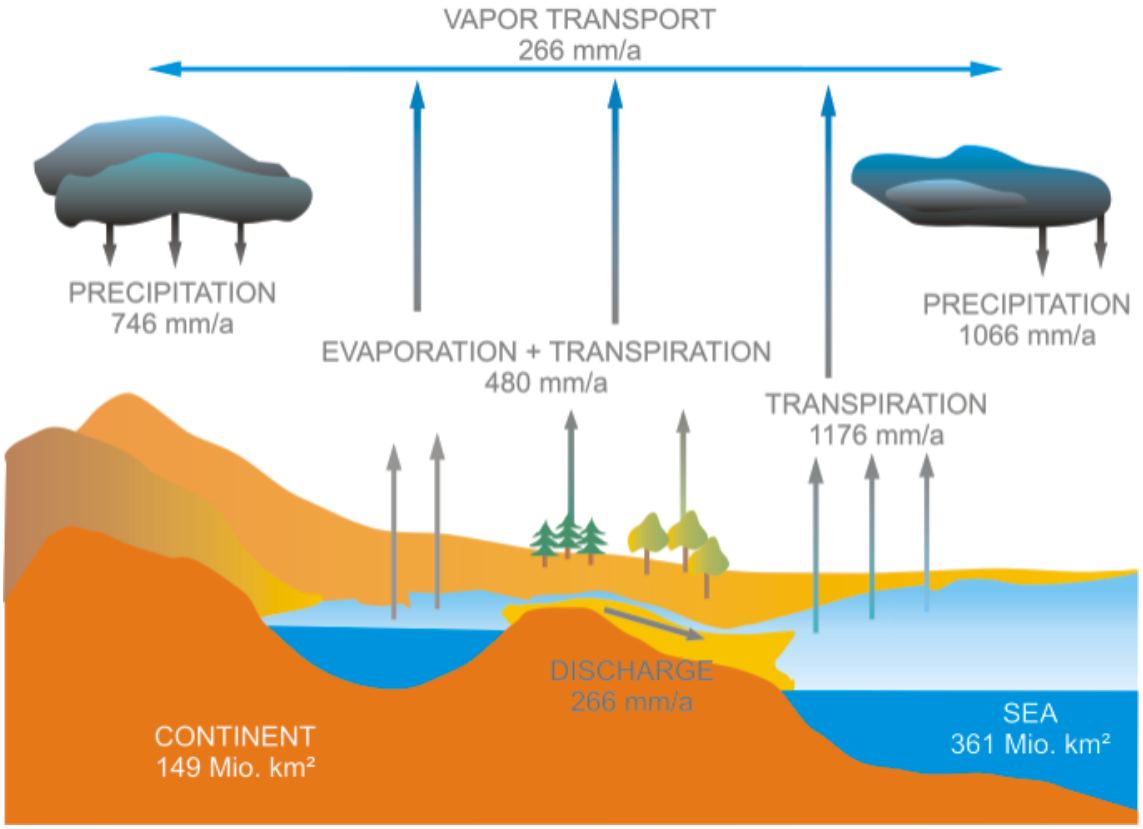

Figure 1.3: Scheme of the average annual global water balance. The figures of the components were taken from Baumgartner (1996).

A portion, depending on the land surface, the available energy and the local meteorological conditions, of the available water (i.e., precipitation P) evaporates E_T (Oke, 1992). The remaining water concentrates for discharge Q, and forms a storage term ΔS. The evapotranspiration directly links the water balance to the energy balance (Kraus, 2004, 2008).
From the complex of hydrological questions arises an important task in the field of hydrology: the quantification of each term of the water balance (cp. Equation 1.1). This is not a trivial task at all because the peculiarity of the driving processes underlies the natural variation, which is smoothed and amplified by anthropogenic factors (Bernstein et al., 2008). The overlapping of these effects leads to variations in the water balance (Baumgartner, 1996). Thus, the geo-temporal dependency of the uncertainties in hydrological models is of great importance for quantifying the water balance. If the hydrological and meteorological information can be more highly resolved by input data obtained by estimation or by real observation, then the uncertainties in the modelling most likely become smaller.
Precipitation turned out to be a component of the water balance, which has great uncertainty in general when it is forecasted or simulated (von Hardenberg et al., 2007; Kronenberg et al., 2013). The uncertainties of small scale, spatio-temporal behaviour of precipitation and the occurrence of extreme precipitation events considerably complicate the assessment and determination of the water balance (Sun and Bertrand-Krajewski, 2013). These uncertainties, among other reasons, result from the high dynamics of water exchange in the atmosphere. For example, when there is a global average of $\sim$1,000 mm precipitation per year with an average of $\sim$25 mm per event, an average of $\sim$40 events could be observed. It is assumed that the atmosphere renews with each event its water content. Then it becomes clear, when these events are spread over one year, that the atmosphere's water content renews every $\sim$9 d on average. This simple example should illustrate the high dynamics of the water exchange. By the same token, strong local influences caused by geographic feedbacks raise the uncertainties.

1.2.1 Precipitation Measurement

Different approaches were and will be developed to observe and determine precipitation as an important part of the water balance on local, regional and global scales (Michaelides, 2008).
Strangeways (2007) divides the major technologies for measuring precipitation into rain gauge, radar and satellite systems. The classical and oldest technology is the rain gauge, which has been developed into a vast array of different types. These can be divided into optical rain gauges, disdrometers and rain gauges, which collect the water in a funnel and measure the water in some way (e.g., manually or electronically by tipping buckets, electronic weighting, capacitance or drop-counting) (Strangeways, 2007). The errors associated with rain gauge measurement are manifold, and they include evaporative loss, outsplash, leveling, an unrepresentative location of the gauge, and the most important error, wind-induced precipitation drift (Sevruk, 1982). Several techniques have been developed to cope with these errors, such as wind shields, turf walls or pit gauges. Instrument and location-dependent correction approaches have also emerged (Richter, 1995; Sevruk, 1982) and have been applied in practise. Thus, the measurement errors can be minimised by the aforementioned methods, but one disadvantage remains when using rain gauge measurements. These data only provide point measurement and therefore do sparsely posses information regarding the spatial distribution of the precipitation.
The highest temporal and spatial resolutions for areal measurement of precipitation are currently achieved by remote sensing systems. These systems can be distinguished by their deployed sensors. Weather radar works on the basis of active sensor, but most satellite systems use passive sensors. An example of experiments that uses passive sensors are the Tropical Rainfall Measuring Missions (TRMM) (Huffman et al., 2007). Passive sensors measure natural thermal radiation (i.e., brightness temperatures). This energy is emitted by all types of surfaces, including snow, rain, clouds, and the Earth's surface (Levizzani et al., 2007). Therefore, the estimation of precipitation by means of passive sensors depends on the minute amount of microwaves energy emitted by the Earth and its atmosphere (Gebremichael and Hossain, 2010). The CloudSat experiment is an example for a satelite-based cloud radar, which is able to measure fine details of different clouds (Stephens et al., 2002). However, as parts (i.e., sensors) of satellites, their

observations cover large areas of the earth. The development of satellite-based systems for estimating precipitation at regional scales is still just beginning. So far, this technology only provides unsatisfactory results at a river basin scale (Thies and Bendix, 2011; Görner et al., 2012). In contrast, ground-based radar-derived QPEs are already practically important and contribute substantially to the process of decision-making in the fields of water and flood risk management (Weigl and Winterrath, 2009; Becker, 2013).

1.3 WEATHER RADAR

The term 'radar' finds its origin in the English phrase describing the technology to detect and observe airplanes: **R**adio **a**ircraft **D**ection **a**nd **R**anging. Today, 'radar' stays for **Ra**dio **D**ection **a**nd **R**anging in a meteorological context. However, in the early days of radar, precipitation was declared as a biased measurement, a detection error. Fortunately, this opinion quickly changed, and the potential of radar technology was recognised. Atmospheric processes can be observed through radar.
Since its introduction, little has changed regarding the fundamental principles of radar. The system uses pulsed energy in the form of electromagnetic waves. These are transmitted by a transmission antenna, which also serves as a receiver (i.e., for mono static antennas). The electromagnetic spectrum for the application of radar in the fields of meteorology is shown in Figure 1.4 and is limited to wavelengths from 1 cm to 15 cm (Rinehart, 2004), with the spectrum divided into seven bandwidth ranges. The particular bandwidths are depicted in Table 1.1. Most of the weather radar systems work in X-Band, C-Band or S-Band. While X-Band instruments are rather ineffective at penetrating through heavy precipitation events, S-Band instruments are rather impractical and expensive due to their large antennas. For these reasons, most of the European weather radar stations use the C-Band technology (Walther, 2007).
As already mentioned, some assumptions are necessary for the meteorological application of radar instruments. These assumptions contribute to a better understanding of the estimation process for precipitation rates based on radar measurements, and they make it clear that the derived measurements are not a direct precipitation observation. Generally, the processing of radar data can be divided into three parts. First, precipitation rates are derived from the measured reflectivities. Second, the error detection and correction are performed. Third, radar data and ground-based point measurements from gauges are merged to correct the bias of the radar data. The processing and measurement-related errors can only be understood by using the often-cited radar equation (Battan, 1973; Doviak, 2006; Bringi, 2001; Battan and Atlas, 1990). For this reason, a simplified derivation of this equation is derived.

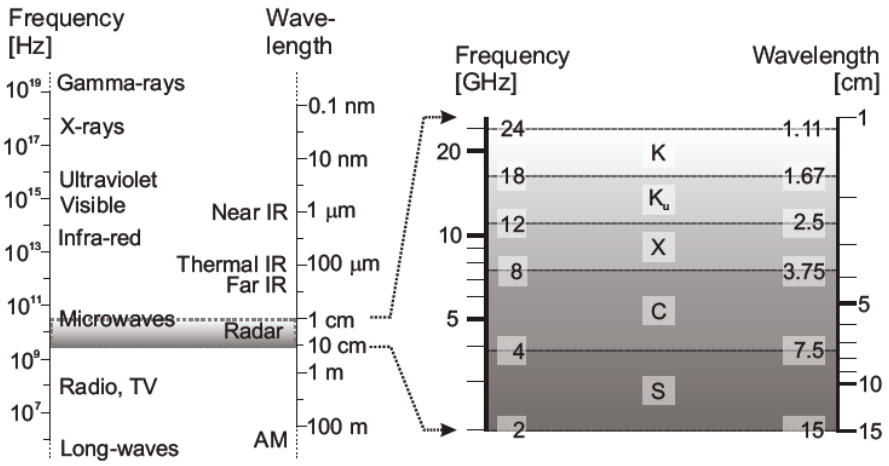

Figure 1.4: Electromagnetic spectrum for the application of weather radar and the respective band designations. The figure was taken from Pfaff (2013).

Table 1.1: Nomenclature for radar band letters with the corresponding wavelength, frequency and application in meteorology (Rinehart, 2004). The table was taken from Walther (2007). The Band letter convention is independent from the symbol convention made in this work.

Band-Designation	**Nominal Wavelength**	**Nominal Frequency**	**Respective meteorological Scatters**
L	30-15 cm	1-2 GHz	
S	15-8 cm	2-4 GHz	large precipitation droplets
C	8-4 cm	4-8 GHz	precipitation
X	4-2.5 cm	8-12 GHz	precipitation and cloud droplets
K_a	2.5-1.7 cm	12-18 GHz	ice, small precipitation and cloud droplets
K	1.7-1.2 cm	18-27 GHz	cloud droplets
K_α	1.2-0.75 cm	27-40 GHz	cloud droplets
V	0.75-0.4 cm	40-75 GHz	cloud droplets
W	0.4-0.27 cm	75-110 GHz	small cloud droplets (up to 95 GHz)

1.3.1 Derivation of the Radar Equation

The derivation of the radar equation at this point is based on certain assumptions without recognition of the possible sources of errors. The derivation considers ideal spherical senders. These are characterised by their isotropic emission of high frequency energy. The energy transmission in space follows the surface of a sphere with uniform power density.
The geometric relationship of Equation 1.2 describes the increase of power density, which depends on the square of the distance. Thus, as its radius r_c decreases, the sphere uniformly allocates the emitted energy on its surface area A.

$$A = 4 \cdot \pi \cdot r_c^2 \tag{1.2}$$

From Equation 1.2, the undirected power density S_u of Equation 1.3 can be derived. It depends on the transmitted power P_S of the sender and the path from the sender to the target r_1.

$$S_u = \frac{P_S}{4 \cdot \pi \cdot r_1^2} \tag{1.3}$$

It is a directed transmission of the radar beam from an antenna, through which the emitted energy is bundled. Thus, the signal does not fill out the whole surface of a sphere, only a particular part of it. This limitation of the area leads to an increase in the power density, but the transmitted energy remains the same. This energy gain due to an antenna is called antenna gain G. The directed power density S_g is defined in Equation 1.4.

$$S_g = S_u \cdot G \tag{1.4}$$

The antenna gain depends on the type of radar antenna. Usually, directed antennas have an antenna gain of 30 to 40 dB. In Equation 1.4, this corresponds to a factor of 1,000 to 10,000.
If the transmitted energy strikes an object, it can be absorbed or reflected. Hence, the targeting does not depend on the power density at the location of the target but on the reflected energy. This energy can be determined by introducing a new variable: the back scattering cross section

σ. This variable is always difficult to determine because it depends on many factors, such as the shape of the target, the surface properties and the material of the target. However, the introduction of the back scattering cross section σ helps mathematically to describe the reflected power at the target P_r. It is shown in Equation 1.5.

$$P_r = \frac{P_S}{4 \cdot \pi \cdot r_1^2} \cdot G \cdot \sigma \tag{1.5}$$

For the derivation of the radar equation, it is usually assumed that propagation of the back-scattered energy also follows a spherical surface. Hence, the same geometric relationships hold for the back-scattering as for the signal transmission from the antennae. The power density at the receiver S_e shows the relationship defined in Equation 1.6, which depends on the reflected power of the target P_r and the path from the target to the receiver r_2.

$$S_e = \frac{P_r}{4 \cdot \pi \cdot r_2^2} \tag{1.6}$$

The measured power at the receiver depends analogously on the power at the target S_e, the power density at the receiver and the effective antenna area A_W. Thus, the power at the receiver P_e can be determined as shown in Equation 1.7.

$$P_e = S_e \cdot A_W \tag{1.7}$$

No antenna is free of energy losses, which is why, instead of the geometric antenna area A_g, an effective antenna area A_W is considered in Equation 1.7. The effective area A_W can be calculated from the geometric antenna area A_g and multiplied by a damping factor K_a, as defined in Equation 1.8. Commonly, K_a is chosen between 0.6 and 0.7.

$$A_W = A_g \cdot K_a \tag{1.8}$$

Thus, Equation 1.9 can be formulated for the power at the receiver P_e.

$$P_e = \frac{P_r}{4 \cdot \pi \cdot r_2^2} \cdot A_g \cdot K_a \tag{1.9}$$

Energy propagates with the speed of light, so every speed relative to it can be ignored for practical reasons. Hence, the distances of radar to target r_1 and target to radar r_2 can be considered to be the same length $r = r_1 = r_2$. The combination of the distances leads to the power at the receiver P_E in Equation 1.10.

$$P_E = \frac{P_S \cdot G \cdot \sigma}{(4 \cdot \pi)^2 \cdot r^4} \cdot A_g \cdot K_a \tag{1.10}$$

It can be shown that the antenna gain G is related to the wavelength λ, as shown in Equation 1.11 (Battan, 1973; Probert-Jones, 1962). A formal derivation of Equation 1.11 is not included here.

$$G = \frac{4 \cdot \pi \cdot A_g \cdot K_a}{\lambda^2} \tag{1.11}$$

The power at the receiver P_E depends on the wavelength λ and can be calculated as shown in Equation 1.12.

$$P_E = \frac{P_S \cdot G^2 \cdot \sigma \cdot \lambda^2}{(4 \cdot \pi)^3 \cdot r^4} \tag{1.12}$$

For the detection of precipitation, the back-scattering cross section σ is of great importance. Basically, it can be determined by means of Mie theory. This theory describes the diffraction of electromagnetic waves at spherical and homogeneous particles. However, as the mean diameter of hydrometeors D does not exceed $\leq$ 15 mm, which is smaller than the usual wavelength of $>$ 5 cm, the back-scattering cross section can be determined by the Rayleigh approximation. This simplifies the scattering relationship and leads to Equation 1.13.

$$\begin{aligned} \sigma &= \tfrac{\pi^5}{\lambda^4} \cdot |K|^2 \cdot D^6 \\ |K|^2 &= \left| \tfrac{\epsilon - 1}{\epsilon + 1} \right|^2 \end{aligned} \tag{1.13}$$

Equation 1.13 shows that the back-scattering cross section, in addition to the droplet diameter, depends on the wavelength and the respective aggregate phase through the permittivity ϵ. Therefore, the factor K was determined for the commonly used frequencies of C- and X-Band of 0.93 for water and 0.2 for ice (Stephens, 1994).
Single droplets are not detected by radar, but a volume is detected. That is why the individual back-scattering cross sections of hydrometeors are summed to within a unit volume of 1 m^3. This leads to summed back-scattering cross sections in which the back-scattering cross section of each particle is integrally considered, as shown in Equation 1.14 with Z as reflectivity.

$$\begin{aligned} \textstyle\sum_{vol} \sigma &= \tfrac{\pi^5}{\lambda^4} \cdot |K|^2 \cdot Z \\ Z &= \textstyle\sum_{i=1}^{n} D_i^6 \end{aligned} \tag{1.14}$$

If droplets are uniformly distributed in the pulse volume V, then the respective volume can be defined according to Equation 1.15 with the angles θ,ϕ, the radius r_V and the parameter h, which depends on the speed of light c_0 and the signal's traveling time τ.

$$\begin{aligned} V &= \pi \cdot \tfrac{r_V \cdot \theta}{2} \cdot \tfrac{r_V \cdot \phi}{2} \cdot \tfrac{h}{2} \\ h &= c_0 \cdot \tau \end{aligned} \tag{1.15}$$

Equation 1.12 is only valid for point targets. Weather radar applications need an adapted form of Equation 1.12. Therefore, Equations 1.13, 1.14 and 1.15 are used to derive an adapted radar equation, as defined in Equation 1.16.

$$P_E = \frac{P_S \cdot G^2 \cdot \lambda^2 \cdot \theta \cdot \phi \cdot h}{2^9 \cdot \pi^2 \cdot r^2} \cdot \sum_{vol} \sigma_i \tag{1.16}$$

Battan (1973) showed that a correction that recognises the antenna pattern is needed. It is assumed that the pattern is of a Gaussian shape, which is generally the case. Thus, Equation 1.17 can be derived by combining Equations 1.14 and 1.16, and this is called the radar equation.

$$P_E = \left(\frac{\pi^3 \cdot P_S \cdot G^2 \cdot \theta \cdot \phi \cdot h \cdot |K|^2}{1024 \cdot \lambda^2 \cdot ln(2)} \right) \cdot \frac{1}{r^2} \cdot \sum_{i=1}^{n} D_i^6 \tag{1.17}$$

The first part of Equation 1.17 contains several radar-specific constants. These can be summarised by the so-called radar constant C. In this manner, Equation 1.17 can be simplified with respect to the reflectivity for weather radar applications, as shown in Equation 1.18.

$$P_E = \frac{C}{r^2} \cdot Z \tag{1.18}$$

The reflectivity spans a wide range of values. Thus, it is usually given on a logarithmic scale, as defined in Equation 1.19.

$$Z_{dB} = 10 \cdot log(Z) \tag{1.19}$$

The radar signal is based on propagation through the atmosphere, and the signal loses strength continuously as it passes through precipitation. This effect is called attenuation of the radar signal. It is an important effect in the case of small wavelengths, for instance, in the X-Band, because the signal is weak in comparison (He, 2011). Therefore, the attenuation of the signal is especially caused by high precipitation rates, dense clouds or a wet radome. The effect was not considered in this derivation of the radar equation, which mainly followed the works of Overeem (2009); Pfaff (2013); Raghavan (2003); Rinehart (2004). More detailed derivation can be found in Collier (1989).

1.3.2 Estimation of Precipitation Rates from Reflectivities

The reflectivity derived in Section 1.3.1 can be brought into a precipitation context through a so-called Z-R relationship, from which one can determine precipitation rates. Marshall and Palmer (1948) used experiments to establish this empirical relationship between precipitation and reflectivity. They stated that the spectrum of rain drops with size approximately follows an exponential function, as shown in Equation 1.20.

$$N(D) = N_0 \cdot e^{-\Lambda \cdot D} \tag{1.20}$$

with $N(D)dD$ = mean number of droplets between the diameter D and $D + dD$ in a unit volume of air and $N_0 = 8 \cdot 10^3$. In Figure 1.5, examples of fitted distribution functions are shown in comparison to the observations of Marshall and Palmer (1948) and data by Laws and Parsons (1943). Figure 1.5 shows that except for small diameters, the fitting of such functions is in fair agreement with observations (Marshall and Palmer, 1948).
The distribution of raindrops is mainly influenced by the growth of droplets due to condensation, sublimation and collision (Straka, 2009; Sumner, 1988). The parameter Λ was derived empirically by Marshall and Palmer (1948), which is given in Equation 1.21.

$$\Lambda = 4 \cdot R^{-0.21} \tag{1.21}$$

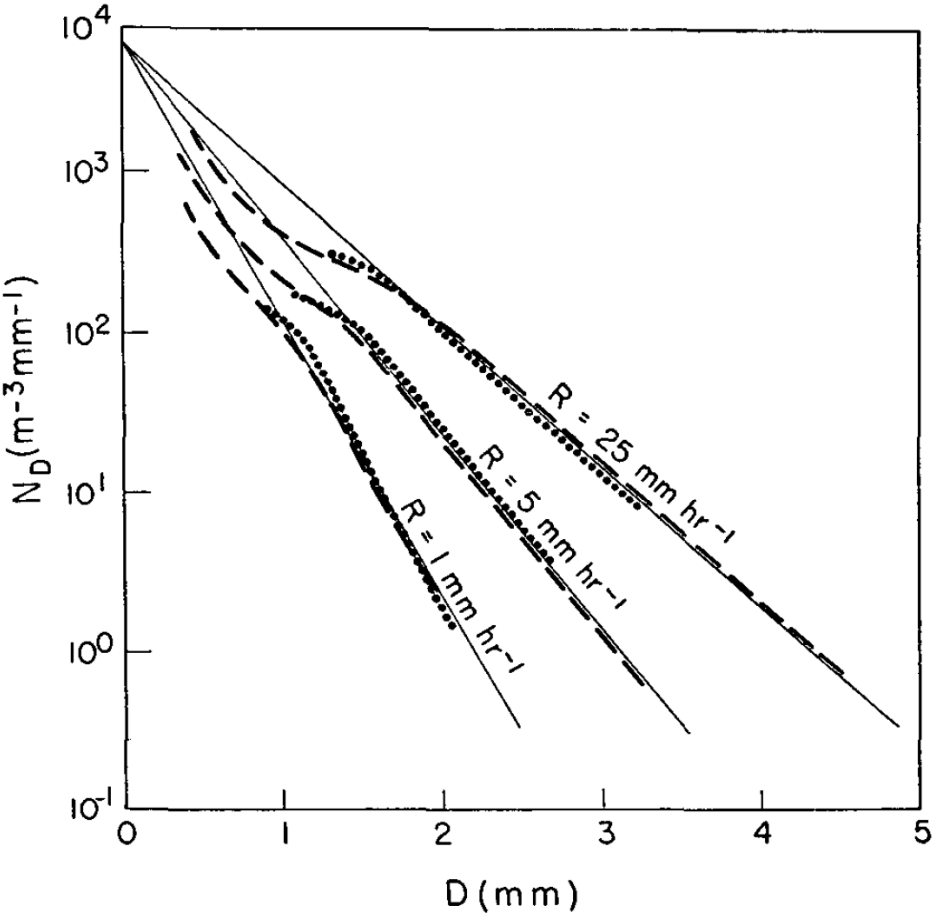

Figure 1.5: Distribution function (solid straight lines) compared with results of Laws and Parsons (1943) (broken lines) and Ottawa observations (dotted lines). The figure was taken from Marshall and Palmer (1948).

The reflectivity is the 6^{th} moment of the droplet distribution $N(D)$ under the assumption of Rayleigh scattering (i.e., when $D \ll \lambda$). It can be defined as shown in Equation 1.22.

$$Z = \int_0^\infty N(D) \cdot D^6 dD \tag{1.22}$$

With the help of the gamma function from Equation 1.23 and the formulated Marshall-Palmer Equation 1.20, a more general Equation for the x^{th} moment of the drop size distribution can by derived, as in Equation 1.24.

$$\Gamma(x) = \int_0^\infty t^{x-1} \cdot e^{-t} dt \tag{1.23}$$

$$\begin{aligned} M(x) &= \textstyle\int_0^\infty N_0 \cdot e^{-\Lambda \cdot} \cdot D^x \\ dD &= \tfrac{N_0 \cdot \Gamma(x+1)}{\Lambda^{x+1}} \end{aligned} \tag{1.24}$$

The reflectivity shown in Equation 1.25 can also be determined. This is in contrast to Equation 1.18, which represents another derivation.

$$Z = M(6) = \frac{N_0 \cdot \Gamma(7)}{\Lambda^7} = \frac{720 \cdot N_0}{\Lambda^7} \tag{1.25}$$

The substitution of Equation 1.21 with Equation 1.25 leads to the Z-R relationship derived by Marshall and Palmer (1948), which is given in Equation 1.26.

$$Z = 296 \cdot R^{1.47} \tag{1.26}$$

This derivation of a Z-R relationship is one of the most famous ones. Several other relationships exist based on derivations and on different experiments with recording gauges and distrometers. Finally, they distinguished the parameters *a* and *b*. Battan (1973) stated in his study that the shape of precipitation is of fundamental importance in addition to the location of the weather radar. Some examples of different parameters of the Z-R relationships are given in Table 1.2.

Table 1.2: Examples of frequently used coefficients of the Z-R relationship

a	b	Reference
296	1.47	Marshall and Palmer (1948)
237	1.5	Atlas and Ulbrich (1977)
200	1.6	Goudenhoofdt and Delobbe (2009)

The thesis of Marx (2007) clearly showed that the Z-R relationship can also be adapted to specific applications. The presented coefficients were not estimated by measurements but by hydrological modelling. This was performed by optimising the coefficients of a precipitation run-off model for a river basin. The basin is located within the range of weather radar.

1.3.3 Possible Errors in the Estimation of Precipitation Rates using Radar

Different factors influence, disturb and introduce errors in the quantitative estimation of precipitation by means of radar. Errors can be classified into two groups. These groups are closely connected to the processing scheme. Errors that occur in the measuring process of reflectivities belong to the first group. The second group of errors are related to uncertainties in the derivation of precipitation rates from reflectivities and derivation of the Z-R relationship. The superposition of uncertanties of these two error groups is responsible for significant differences between radar-derived precipitation and gauge data (Wilson and Brandes, 1979).

1.3.3.1 Measurement of Reflectivities

Potential sources of error can be observed in the radar instrument itself. In the literature, such errors are often referred to as incorrect calibration of the instrument, which may lead to systematic errors in the measurement of reflectivities. However, calibration cannot correct all hardware-related errors. For example, errors such as radar rings can occur (Hengstebeck et al., 2010). After calibration, which should take into account local reference measurements (Wilson and Brandes, 1979), there are several possibilities for hardware-independent errors, which cause abnormal precipitation measurements. These errors can have the following causes:

1. Blockage of the radar beam by objects of a significant height, such as large buildings in the vicinity of the radar station. These obstacles lead to so-called spikes in the radar picture because information at their lee sides is lost. Affected pixels can be detected and corrected by a geometric optic approach based on a interception function (Bech et al., 2003).

2. Detection of static or moving non-meteorological targets. These can be planes, wind turbines, cranes or even swarms of insects (Knott, 2004; Marx, 2007; Toth et al., 2011). Typically, these so-called static clutter items are removed by a clutter map. Non-static clutter (like swarms of insects or increased air traffic densities) can be detected and removed by means of statistical filters and dynamic elevation maps (Fornasiero et al., 2006; Bartels et al., 2004).

3. Abnormal propagation of the radar signal, which is sometimes called 'anaprop' (Doviak, 2006). This phenomenon can be observed when the refractive index is modified by changes in the pressure, water vapour or temperature gradients of the atmosphere, which can be caused, for example, by a temperature inversion. Several techniques exist for the detection and correction of anaprop, such as the method of Alberoni et al. (2001).

4. Build-up of water films on the radome (Wilson and Brandes, 1979).

5. Attenuation of the signal due to dense clouds and precipitation. The attenuation depends on the atmosphere's water content. Under this restriction, it can be stated that heavier rains increase attenuation, whereas clouds with smaller water content lead to less attenuation. Additionally, differences between ice and liquid particles can be observed. In comparison, attenuation by ice particles can almost be neglected. However, experience has shown that large amounts of melting ice or hail particles can result in large increases in reflectivities and can therefore cause significant attenuation.

6. Bright Band, which may occur by the transition from snow and ice particle into rain in the atmosphere. The effect can be found in the melting layer, which reaches the mid latitudes up to 4 km altitude. This effect is first caused by the extremities of a snowflake melt. The available water creates a covering film before the particle implodes to form a droplet. Due to the high conductivity of water and the seemingly large volume of the water-coated snowflake, the reflectivities significantly increase Michaelides (2008).

Some of these errors can be observed in Figure 1.2. Furthermore, the figure depicts errors that arise by temporal aggregation of the precipitation rates of a multi-sensor composite.

1.3.3.2 Uncertainties of the Z-R relationship

The experimentally derived Z-R relationship for the estimation of precipitation rates from reflectivities is determined by the two parameters *a* and *b*. The derivations of these parameters often require assumptions, which necessarily lead to uncertainties. Thus, the derivation by Marshall and Palmer (1948) starts from the premise that the scanned volume of air is uniformly filled by precipitation particles, that the drop-size distribution follows an exponential function, which also could be bimodal if there is a difference between stratiform and convective precipitation, that rain drops posses a spherical and homogenous shape and that all particles have the same aggregate state (Marx, 2007). Also Wilson and Brandes (1979), concluded that the reasons for erroneous estimation of precipitation rates by means of radar are related to differences in the relationship between reflected energy and precipitation rate, the shape and change of the aggregate state of the precipitation particles within the process of falling, abnormal signal propagation and attenuation in the atmosphere. For these reasons, it is usually recommended to use an adapted Z-R relationship that considers the local circumstances and hardware configurations. The coefficients should at least be chosen so that they depend on the type and strength of the particular precipitation events.

Table 1.3: Examples of adapted coefficients for the Z-R relationship

a	b	Precipitation Type	Reference
140	1.5	Drizzel	Battan (1973); He (2011)
250	1.5	Widespread rain	Battan (1973); He (2011)
500	1.5	Thunderstorm	Battan (1973); He (2011)
140	1.6	Drizzel	Strangeways (2007)
180	1.6	Widespread frontal rain	Strangeways (2007)
240 or 500	1.6	Heavy convective showers in the UK or alpine regions	Strangeways (2007)

Table 1.3 illustrates the role of precipitation type in the Z-R relationship. Obviously, the location and the climatological conditions at the radar site must be considered. Hence, tropical conditions and extreme precipitation events are particularly problematic for the quantitative estimation of precipitation rates (Palmer, 2010).

1.3.3.3 Merging Techniques

Radar data have high spatial and temporal resolution, but the data also posses several possible errors, which are related to the measuring principle or the assumptions made for the estimation of precipitation rates (Berndt et al., 2014). The application of uncorrected precipitation rates derived by radar in hydrological or climatological applications therefore is not acceptable (Berndt et al., 2014). For this reason several approaches have been developed to correct the data. Usually, the radar information is merged with gauge data. That is why these approaches are also called merging techniques. The outcome of this processing is a better estimate of the precipitation product for the considered domain. The techniques always involve a comparison between gauge data and the corresponding radar pixels. For high temporal resolutions it is recommended to use, instead of one radar pixel, the mean from the nine pixels closest to a gauge (Goudenhoofdt and Delobbe, 2009). Especially for solid precipitation such as snow, the wind drift can be up to 20 km. This must be considered in a comparison (Mittermaier et al., 2004). The effect can be neglected for longer periods. Likewise, a critical and close inspection of the representation of the gauges is important. These should represent a fairly large region (Lang, 1997). Aniol et al. (1980) showed that even gauges with small distances between them have differences on hourly and daily bases of up to 10 $\%$. Therefore, it is important to question the quality of the gauge data. In the following section, the most popular merging techniques are presented.

Mean field bias correction (MFBC) assumes that precipitation values derived from radar data are biased by a identical distributed bias. The bias can be caused by incorrect hardware calibration or insufficient coefficients of the Z-R relationship (Steiner et al., 1999). The bias B_{MFBC} of the precipitation rates can be removed as shown in Equations 1.27 and 1.28.

$$Z = a \cdot B_{MFBC}^{-b} \cdot R^b \tag{1.27}$$

$$B_{MFBC} = \frac{\frac{1}{n} \cdot \sum_{i=1}^{n} S_i}{\frac{1}{n} \cdot \sum_{i=1}^{n} \Re_i} \tag{1.28}$$

The exponential relationship between reflectivity Z and precipitation rate R can be used to correct the mean difference (i.e., bias) between all n radar-derived precipitation rates $\Re$ and gauge measurements S. The approach is regarded as one of the simplest. Its application led to several different processing scenarios on a daily basis to provide satisfactory Root Mean Square Errors (Goudenhoofdt and Delobbe, 2009).

Range-dependent adjustment (RDA) proceeds on the assumption that the quotient between radar and gauge depends on the distance r from the radar station. This assumption is reasonable because the elevation angle of the radar beam is larger than 0°, so the signal reaches higher parts of the atmosphere as it propagates farther from the radar station (i.e., the range effect) (Raghavan, 2003). Likewise important is the aforementioned attenuation of the signal, which is proportional to the path from sender to target and back. The quotient between radar and gauge is calculated on a logarithmic scale through a 2^{nd} degree polynomial. The coefficients r,p,o of the polynomial are approximated by the method of least squares. The range-dependent correction factor B_{RDA} can be determined as defined in Equation 1.29.

$$log(B_{RDA}) = l \cdot r_{RDA}^2 + p \cdot r_{RDA} + o \tag{1.29}$$

Static local bias correction and range dependent adjustment (SRD) claims to correct for visibility effects (Goudenhoofdt and Delobbe, 2009) . It is applicable for annual data sets. More specifically, it assumes the existence of an annual long data set of observations. The processing consists of three parts. First, an MFBC is deployed for aggregated 24 h rates. In the second step, the annual biases between gauges and radar measurements are calculated (i.e., Static local bias (SLB)). Then, this information is interpolated by means of appropriate spatial interpolation techniques and deployed in a manner similar to MFBC for the radar data. In the third and last step, an RDA is applied on a daily basis with the correction factor from the SLB of the last year, as shown in Equation 1.30. The comparison of 24 h precipitation rates showed that the performance is as good as some more sophisticated approaches (Goudenhoofdt and Delobbe, 2009).

$$B_{SLC} = B_{MFBC} + B_{SLB} + B_{RDA} \tag{1.30}$$

Brandes spatial adjustment (BRA) is a another approach to correct the spatial bias of radar data (Brandes, 1975). For this adjustment, one correction factor is calculated for each gauge. The method follows the objective analysis of Barnes, which is a convergent weighted-averaging interpolation scheme (Barnes, 1964). Through the scheme, a spatial correction field can be calculated on the basis of negative exponential weighting. The weighting factors w depend on the distances d of a pixel from the gauges and one empirical factor u. Equation 1.31 defines how to calculate the correction field B_{BRA}.

$$\begin{aligned} B_{BRA} &= \frac{\sum_{i=1}^{n} w_i \cdot (\frac{S_i}{\Re_i})}{\sum_{i=1}^{n} w_i} \\ w_i &= e^{\frac{-d_i^2}{u}} \end{aligned} \tag{1.31}$$

The coefficient (i.e. empirical factor) u serves as a smoothing parameter within the interpolation scheme, as in the case of Inverse Distance Weighting. The smaller the parameter, the more details remain from the original data (Brandes, 1975). Goudenhoofdt and Delobbe (2009) defined this factor as the mean station density, which can be derived from the number of given stations divided by the area of the domain. The results of their study show that the applied approach on a daily basis led to significantly better results than BRA.

Geostatistical approaches are a large group of methods, which through spatial interpolation and on the basis of point samples generate a random field. The spatial distribution of precipitation in this case is considered as such a random field.
A comprehensive overview of the principles and assumptions of geostatistical approaches can be found in Wackernagel (2003); Goovaerts (1997). One thing that all of these approaches have in common is that they require the definition of a variogram, which describes the spatial variability of the precipitation field.
For the merging of radar and gauge data, currently one approach finds preferential application: External Drift Kriging (EDK). The approach allows the interpolation of a variable under consideration of additional variables. The main variable is observed data from gauges, and radar data are handled as background information. The use of EDK leads to fair agreement on a daily basis between gauge and radar precipitation fields (Velasco-Forero et al., 2009). This is also supported by Verworn and Haberlandt (2011), who showed that the approach led to good results for 15 single storm events and the corresponding variograms in different configurations (i.e., different combinations of additional variables such as topography, precipitation type or reflectivities instead of precipitation rates). The authors emphasised that the quality of the obtained precipitation field most notably depends on the empirical variogram (van de Beek et al., 2011). The determination of a variogram occasionally turns out to be difficult, especially in study regions that are located in high mountain ranges with sparse networks of gauges (Holawe and Dutter, 1999). Likewise important are the uncertainties of a regionalised variable (i.e., interpolated precipitation) at high temporal resolutions, which are associated with its dynamics (cp. Section 1.2).

Beside the aforementioned approach, other methods exist. They are mixtures or extensions of the already introduced ones (Ehret et al., 2008; García-Pintado et al., 2009).
The remaining variance between gauge and radar data after a merging mainly is the consequence of different measurement principles, the drop spectrum and some other factors (Lang, 1997). Even after correction of the aforementioned known errors, it should not be forgotten that radar measurement is only a 'snapshot', which is normally updated with a 5 *min* interval.

1.3.4 The RADOLAN Project of the DWD

Despite the obvious disadvantages of estimating precipitation by radar, several complex processing schemes have been developed to increase the quality of QPE products. The quality assessment and growing demands of highly resolved data sets in practise and in science have led to national and international projects for generated QPEs over large areas (Smalley et al., 2014; Michelson and Koistinen, 2000). Especially short time forecasting of potentially dangerous hydrometeorological situations was the motivation for continuous progress in the field of QPEs. These developments have reached a state of on-the-fly processing and immediate online availability of QPEs for risk assessment tasks (Becker, 2013; Weigl and Winterrath, 2009). For this reason, almost 10 years ago, the DWD started the operational service RADOLAN.
RADOLAN is a acronym -'for a comprehensively and operationally generated data set based on a radar online merging approach', which was developed to process real-time radar and recording gauge data from the DWD. The obtained data are available in high spatial (i.e., 1 km) and temporal (i.e., for the rw-product which claims to be one of the end products of 1 h) resolutions for an extended region of Germany.
The quality of the radar-derived precipitation data without additional merging with point measurements (i.e., recording gauges) is insufficient for quantitative applications (i.e., in the fields of water management), as is shown in the aforementioned Section 1.3.3.3 (Weigl and Winterrath, 2009). For this reason, the RADOLAN algorithm attempts to combine the advantages of two different measuring procedures. On the one hand, direct local point measurement is used to acquire precipitation near-ground, and on the other hand, indirect measurement is used to describe the spatial precipitation distribution of the radar picture (Lang, 1997). The achieved synthesis of gauge and radar data is used to build QPEs.

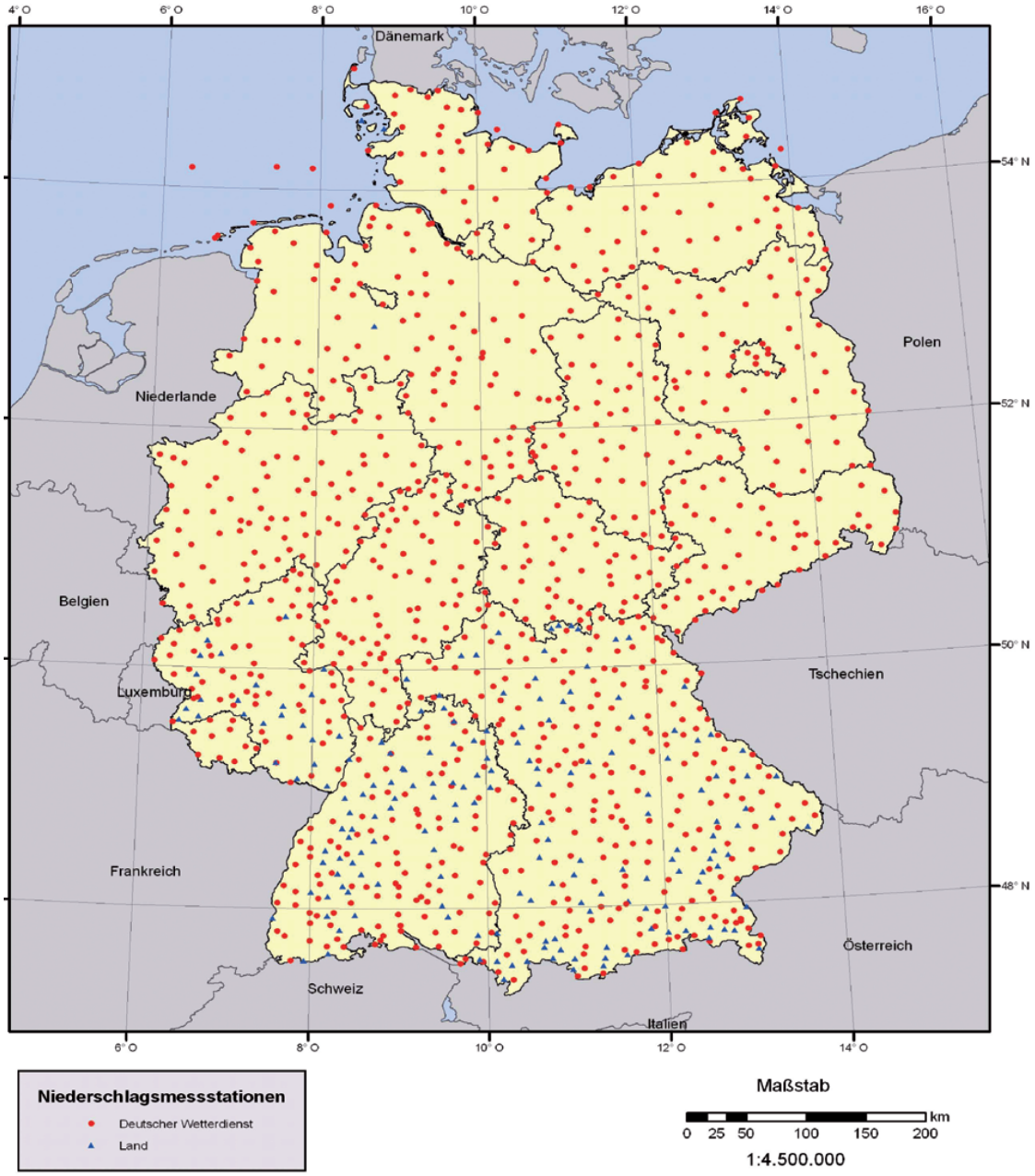

Figure 1.6: Gauge networks of recording gauges of the German Weather Service (DWD) and of some federal states (Land) with a data transmission interval of 1 h. The figure was taken from Weigl and Winterrath (2009).

Comparable precipitation products for other regions include BALTRAD for the Baltic Sea (Michelson and Koistinen, 2000) and the NCEP Stage IV product for the United States of America (Smalley et al., 2014). The underlying radar networks possess more than 30 and 200 weather radar stations. Their data likewise are mainly processed and obtained for hydrological applications (Walther, 2007).

The RADOLAN products are based on a network of 16 C-Band radar stations, the precipitation gauge networks of the Federal States of Germany and the recording gauge network of the DWD (Weigl and Winterrath, 2009). The respective networks are depicted in Figures 1.6 and 1.7. Figure

1.6 shows the density of recording rain gauges, which are taken into account within the operational processing. These gauging stations are almost equally spatially distributed. The network possesses a comparable high density, but due to the equal spatial distribution, mountain-induced features of the spatial precipitation distribution only find a limited representation in the gauge measurements. Figure 1.7 shows the locations of the radar stations and their beam coverages in Germany. The high network density leads to a redundancy of radar observations for over 50 % of the covered area.
'Precipitation scans' at 5 min intervals of the weather radar stations are taken into account for the quantitative precipitation estimation. The radar stations have a range of 125 km. The recording gauge networks of the DWD and the Federal States of Germany include a total of 1,100 gauges. These transmit their recordings in 1 h intervals for online merging. Additionally, up to 200 recording gauges from the adjacent states can be used for processing, primarily to reduce interpolation errors in the periphery of the composites.
The processing of the radar data consists of various sub-steps of quantitative precipitation estimation, which take place before the actual merging is performed. The most important steps are listed below, and they are described more deeply in the RADOLAN documentation by Bartels et al. (2004).

1. Correction of orographic shadowing
2. Quantitative composite calculation from the different weather radar stations in Germany
3. Statistical clutter suppression
4. Smoothing of gradients
5. Pre-merging with factors from gauges and radar on the bases of maximal detected precipitation

The correction of the bias is deployed for recording gauges and the nine radar pixels closest to the gauge. From these nine pixels, the differences and quotients between the respective pixel and gauge values are calculated. The factor mostly corresponding to one or smallest difference of these nine pixels is then used for interpolation. At each location (i.e., gauge) one factor (difference) is identified, which is interpolated for all gauges over the whole composite. The choice of technique (differences or quotient) is determined by a subset of recording gauges. These rain gauges are not used to determine the aforementioned factors (differences), but to validate the interpolated fields. The smallest absolute difference over all recording gauges for validation is taken into account for an objective choice of a proper merging technique at one time step (Bartels et al., 2004). In this manner, two different merging approaches can be operationally used.
As the processing chain from the measuring of reflectivities to the final QPE derivation is a complex procedure, many products are generated at each processing step. These products are put into an archive and stay available on demand (DWD, 2009).
Weigl and Winterrath (2009) stated that, when the radar radius is 100 km, the usage of 40 to 60 recording gauges had been successfully proven with a sufficient quality for the obtained QPEs used in water management tasks.
This is also supported by Goudenhoofdt and Delobbe (2009) and their investigation concerning different techniques of merging radar and gauge data.
The DWD has prospects for different future extensions of their radar and gauge networks. Furthermore, closer cooperation with adjacent states, such as France, Belgium and Switzerland, could help to cover the territory of Germany in a better manner by radar. In addition, the spatial extension for Europe of the RADOLAN products with the name RADOLAN-ME for water management applications is available and will be further developed.

Figure 1.7: Network of C-Band weather radar stations of the German Weather Service (DWD) in Germany and their beam coverages. The figure was taken from Weigl and Winterrath (2009).

2 PUBLICATIONS

In the original submitted cumulative dissertation all peer-reviewed publications were included in Chapter 2, which are subsequently merely mentioned.

2.1 CLASSIFICATION OF DAILY PRECIPITATION PATTERNS ON THE BASIS OF RADAR-DERIVED PRECIPITATION RATES FOR SAXONY, GERMANY

Kronenberg, R., Franke, J. and Bernhofer, C.: Classification of daily precipitation patterns on the basis of radar derived precipitation rates for Saxony, Germany, Meteorologische Zeitschrift, 2012, Vol. 21, No. 5, 475-486, DOI: 10.1127/0941-2948/2012/0343.

2.2 COMPARISON OF DIFFERENT APPROACHES TO FIT LOG-NORMAL MIXTURES ON RADAR-DERIVED PRECIPITATION DATA

Kronenberg, R., Franke, J. and Bernhofer, C.: Comparison of different approaches to fit log-normal mixtures on radar-derived precipitation data, Meteorological Applications, 2014, Vol. 21, No. 3, 743-754, DOI: 10.1002/met.1402.

2.3 A METHODE TO ADAPT RADAR-DERIVED PRECIPITATION FIELDS FOR CLIMATOLOGICAL APPLICATIONS

Kronenberg, R. and Bernhofer, C.: A methode to adapt radar-derived precipitation fields for climatological applications, Meteorological Applications, 2015, DOI: 10.1002/met.1498.

3 SUMMARY AND MAJOR FINDINGS

The proposed objectives of this work (cp. Section 1.1) are considered next. The major findings of the manuscripts from Chapter 2 are summarised.
The assessment of precipitation products can be divided into two parts, as performed by Görner et al. (2011, 2012). The first publication consists of a temporal analysis, and in the second one, the spatial limitations of QPEs are discussed. The temporal investigation is the easier part. It considers a comparison between rain gauges and radar pixels. The spatial validation is more complicated, for there is no reliable product (i.e., observed data) available to compare to the RADOLAN rw-product at a spatial resolution of 1 km (Görner et al., 2012). Therefore, an indirect method is proposed for the assessment of the goodness-of-fit of mixture distributions over different spatial scales (cp. Section 2.2).
The temporal validation showed the following results. The mean of the 9 pixel box was not calculated (cp. Section 1.3.3.3). Rather, the nearest pixel to one gauge was taken into account. The calculated correlations for the recording gauges at hourly resolution are always higher than 0.90, which is an expected level of agreement and indicates a reasonable linear relationship between the two measuring systems. The high correlations can be explained by the fact that most likely, the same recording gauges were used for the merging procedure. However, due to temporal aggregation and a different measuring network of non-recording gauges, Hellmann gauges (Richter, 1995)), the correlation decreases to a limit that should be considered to be the lower limit in terms of a reasonable linear relationship (i.e., $> 0.67\%$ for significance (Giles, 2002)). Consequently the temporal assessment of the product showed that applications for long-term or extreme precipitation climatologies of the RADOLAN rw-product are not recommended, but they were also not intended by the RADOLAN authors (Weigl and Winterrath, 2009).

1. Can spatially highly resolved daily precipitation fields be robustly classified into groups of similar spatial patterns?

The methods of multivariate statistics include many reliable algorithms for classifying data (Wilks, 2011; Schönwiese, 2013). The major problem for the classification of QPEs in general and in this thesis is their high spatial resolution. The resolution makes the processing expensive in terms of computer resources and the large density of precipitation information. Therefore, the high variability of precipitation may serve to obscure and limit classification. Usually, classes contain all sample points (i.e., objects) of a data set. However, the classification can be based on fuzzy or hard clustering. In the first case, an object belongs to a certain degree to all classes, and in the second case, each object belongs to one and only one class (Höppner, 1999).
The methods applied, such as cluster analysis and unsupervised neural networks, are able to identify robust classes (i.e., hard clustering), whereas Principle Component Analysis (Pearson, 1901) leads to rather obscure results, which could not be associated with plausible interpretations. The later method likely was corrupted or influenced by measurement errors rather than by

the actual precipitation information. However, in terms of neural networks and cluster analysis, a robust classification of a reliable (i.e., representative) sample size can be performed.

2. What relationships exist between classes of similar daily precipitation fields, seasons and synoptic situations?

Of course, relationships exist, and they were expected because precipitation depends on seasons and on the particular state of the atmosphere (Sumner, 1996). That is why the question focuses on the strength of the impact and the statistical significance of specific properties.
Precipitation is a very complex element, which is influenced by large-scale (e.g., seasons and weather patterns) as well as small-scale features (e.g., regional topography and land use). For this reason, the strongest dependencies could be observed between the classified patterns and the moisture content of the air and the prevailing wind direction. Seasons play a less significant role for the particular patterns. A bit stronger are the observed relationships of the patterns of air pressure at the 500 hPa level followed by air pressure at the 950 hPa level.

3. Do precipitation patterns improve the fitting of distribution functions on radar-derived precipitation data?

The results of Section 2.2 clearly show that parameters derived by classification, either by neural networks or by cluster analysis as initial guesses, which were then optimised by a Maximum Likelihood approach, show a better performance for large spatial resolutions (i.e., < 4 km) of the considered radar product. They performed best in comparison to simple log-normal distributions in terms of the Kolmogorov-Smirnov tests. However, it should be noted that simple gamma distributions perform almost equally well at these spatial resolutions.
In conclusion, the classified precipitation classes could significantly improve the performance (i.e., goodness of fit) of the log-normal distributions. However, gamma distributions, which have fewer parameters, are also a good choice for modelling the daily precipitation rates in this particular domain.

4. How do the fitted distribution functions perform over different spatial scales?

Several parametric distribution functions can be deployed to describe the daily spectrum of precipitation time series (cp. Section 2.2). These functions are fitted to orderless values of former time series of point measurements to parameterise their probability distributions. Due to the central limit theorem, it was more or less expected that all distributions, theoretical and empirical, would converge to a normal distribution by simple aggregation of the sample points when their variance is finite and positive (Storch, 2001). For this case, the spatial correlation of precipitation must be neglected because the central limit theorem theoretically holds only for independent variables.
Aggregation may be either over time or over space. For the test of goodness-of-fit, the spatial aggregation was investigated. The results support the predictions of the assumed central limit theorem. All applied functions with increasing spatial resolution perform worse in terms of Kolmogorov-Smirnov tests for the study region.
The analysis of the fitting qualities shows unexpected behaviour. At the smallest scale of 1 km pixel edge length, the portion of good functions (i.e., those with H_0 not rejected by the Kolmogorov-Smirnov Test) is smaller than for 2, 3 or 4 km resolutions. This finding contradicts with the initial statement of a good description by the chosen parametric distribution function for point measurements. However, because the QPE used here is derived by radar, it must be considered in a radar context. For example, NEXRAD has a spatial resolution of 4 km (Anagnostou and Krajewski, 1998), Overeem et al. (2009, 2010) used a radar product with 2.4 km resolution, and the OPERA radar composite has a resolution of 2.5 km (Chang, 2012). The spatial properties of these products together with the results presented here suggest the use of the RADOLAN rw-product with a spatial scale of at least 2 or 3 km for daily precipitation fields.

5. How can reappearing errors due to temporal aggregation of QPEs be detected and corrected for long-term climatological applications?

The correction of errors within an already processed QPE product is a difficult task and depends on the detection of incorrect precipitation information. These errors are obvious by visual investigation, but they need to be detected and corrected or at least excluded objectively in an automated way to fulfil the practical requirements of an online processing scheme. For this reason, the errors can be divided into two groups.
The first group consists of errors that are obviously wrong in terms of a natural spectrum of precipitation. This spectrum might be defined over time (i.e., errors within time series), over space (i.e., errors in raster over a certain domain at a certain point of time) or spatio-temporally (i.e., a combination of both). Nevertheless, errors can easily be detected, and in this case they can be considered as outliers of the particular spectrum (i.e., the empirical distribution of precipitation rates over space, time or both). The particular pixels should be excluded from the data set.
The second group of errors is more difficult to detect. These errors lay within the aforementioned spectrum of precipitation, but they form artificial patterns that, when observed by hand, obviously arise from the merging of different radar stations (i.e., multi-sensor composite). Other errors arise from processing and measuring peculiarities. These errors should not be excluded; they should be adapted because they may have a large spatial extent in the study region. Additionally, the values may be biased, but they are not completely wrong. Thus, they must be adjusted to compensate for the bias. The chosen approach for this task takes into account a reasonable relationship between elevation and precipitation, which lasts for periods of one year or longer. According to this assumption, the precipitation spectrum follows the elevation or at least presents an almost linear relationship between them, which can be expressed by a linear regression with a certain portion of explained variance. The considered QPEs of this work are corrupted by certain errors, which impair a direct climatological analysis of the precipitation field. The presented approach therefore consisted of several steps to correct the precipitation field for climatological applications. The errors are statistically detected and excluded. The exclusion scheme consists of an inter-quartile outlier procedure that depends on three empirical parameters. These could be determined for the particular data set by means of simulation and optimisation.
False precipitation information, which cannot be statistically detected because it is within a plausible range of precipitation in the domain, is adapted by taking elevation features into account by linear regression. Finally, further merging is performed using a differences method on the basis of climatic rain gauges (Weigl and Winterrath, 2009).
The presented approach is scale-free (however, a spatially independent approach is only valid for precipitation sums over yearly or larger periods), and it is transferable, but the derived parameters are considered to be bound to the particular domain. That is why they must be determined again for other study regions. Nevertheless, it seems that the obtained parameter f_u is not very sensitive; the obtained values range between 2 and 3 and therefore are close to the value of 3 proposed by Eischeid et al. (1995).

6. How are radar-derived long-term precipitation fields different from conventionally interpolated fields based on rain gauge data?

The investigated interpolated precipitations fields based on rain gauge data either receive their spatial variability from variograms as used in the Kriging procedures (Wackernagel, 2003) or from additional orographic information, as in the multivariate regression procedure (Rauthe et al., 2013). The pattern comparison shows that the degree of spatial heterogeneity of fields derived from radar data with the presented approach is as high as for the conventional interpolated fields.
It must be stated that additional information regarding the elevations includes the features with the highest impact on spatial variability at longer time scales, as was investigated. This holds for the interpolated fields (i.e., QPE) with and without and the radar-derived information in this work. The presented approach accounts for the elevation just to correct the radar pixels corrupted by false precipitation information or errors. Therefore, the achieved spatial variability of the long-term precipitation fields is likewise not a measured value but an estimated one.
Despite good correspondence and supplementation of the radar and rain gauges, there are significant differences in the measuring principles, which lead to more or less significant differences

in the precipitation rates between rain gauges and radar. The rain gauge area of a conventional daily non-recording gauge in Germany is 200 cm^2 (Sevruk, 1974). Thus, the area is a multiple of $50 \cdot 10^6$ smaller than the projected area of a radar pixel (i.e., 1 km^2) (Riedl, 1986; Lang, 1997). Additionally, even radar pixels measured in polar coordination are not consistent at all. The raw data of a radar usually comes in polar coordinates. Accordingly, a projection on a regular raster becomes necessary. Therefore, the radar pixel value varies depending on the distance to the radar station up to a factor of 100 (Riedl, 1986).
Although the radar-derived fields possess more information regarding the spatial variability than gauge-based products, this information is corrected and has to be interpreted with consideration of the known weaknesses of the data and the processing scheme.

4 CONCLUSIVE OUTLOOK AND PERSPECTIVES

The climatological analysis of precipitation products derived from radar data was neglected, as the available data were collected over a period too short for the WMO requirements of climatological purposes (World Meteorological Organization, 2008). The period of available and comprehensive radar data is too short, especially for Germany (Becker, 2013). Nevertheless, a few climatologies already have been derived, especially concerning extreme precipitation events (Allen and DeGaetano, 2005; Overeem, 2009; Overeem et al., 2010). These types of climatologies are of special interest in several dimensioning and construction tasks in the field of water management (DIN, 2008; DWA, 2006). However, the processing of the data has certain limits due to the measurement principles of radar (cp. Section 1.3.3). As a consequence, the processed data are now specialised for certain applications.

It becomes obvious through the presented results that the processing of radar data depends on the application purpose and the temporal scale. Thus, a change in the respective algorithms becomes necessary with respect to the geo-temporal scales.

Scale-free and inappropriate processing is therefore a future challenge that the hydro-meteorology community must face. In contrast, the demand for highly resolved data sets continuously increases with an equally strong claim regarding the adequate quality of the data. Ground-based point measurements and dense gauge networks for recording are needed, as well as non-recording (i.e., manual) rain gauges in different temporal resolutions for processing radar data. That is why, in addition to scale-free processing, the question of an optimal gauge network for indispensable merging arises. The three technologies used to measure precipitation complement each other in the task of quantitative precipitation estimation (cp. Section 1.2.1). Additionally, satellite-based sensors, systems and algorithms will gain more relevance (Thies and Bendix, 2011). As this occurs, the procedures and techniques used to obtain multi-sensor and instrument QPEs by merging observed data of different measuring systems (i.e., from satellites, radars and rain gauges) must be refined.

As QPE quality increases, assimilation routines should be adapted into dynamic meteorological and hydrological models by means of Kalman filters or appropriate variational approaches. The use of dual-polarisation measurements will allow for more accurate QPEs, and refractivity data could give some information regarding humidity 30 to 60 km around the radar station. Webb (2013) concluded that even higher spatial resolutions of 100 m pixel size are imaginable. All of these potentials imply renewals of radar instruments but may cause inconsistency through instrument changes within radar-derived precipitation time series.

The completion of this thesis is marked by the start of a new project in February 2014 at the DWD on the analysis of precipitation climatologies with radar-derived data. It was recognised by experts and officials that this field needs more research and that the development and testing

requires time for the appropriate methods to reach maturity suitable for operational applications. The latest developments in the radar meteorological community show that the focus is shifting from the processing of radar data for water management tasks (Bartels et al., 2004; Weigl and Winterrath, 2009) to climatological applications (Becker, 2013). The development and validation of highly resolved composite products (i.e., QPEs) (Chang, 2012) shows that the current state of the art still has considerable uncertainties pertaining to the following factors:

1. observation, estimation and simulation of the regional and global water balance,
2. the analysis of extreme precipitation events
3. the assessment of small-scale precipitation variability

Radar-derived data are considered to contribute significantly to a better understanding of these issues (Becker, 2013). Considering this shifting focus, future contributions should aim for the processing of radar data that is independent of the temporal scale and the considered application. Therefore, the research focus must be extended because future QPEs should be consistent over space and time and should be applicable for hydrological tasks as well as for climatological applications. For this reason, further challenges can be found in the processing of multi-sensor data and in the development of procedures that can appropriately suppress known errors, as well as the development of integrated data validation methods that consider not only the statistics of the derived data sets but also their performance in terms of impact modelling. This includes validation with multidimensional data sets or single time-series transformed data by deploying the data in calibrated models. In this manner, redundancies of sensors can be effectively handled, and with the help of physical models, correlations between variable can be used to detect faulty data. Additionally, uncertainty analysis must be more strongly integrated into data validation.

BIBLIOGRAPHY

Alberoni, P. P., Andersson, T., Mezzasalma, P., Michelson, D. B., and Nanni, S. (2001). Use of the vertical reflectivity profile for identification of anomalous propagation. *Meteorological Applications*, 8(3):257–266.

Allen, R. J. and DeGaetano, A. T. (2005). Considerations for the use of radar-derived precipitation estimates in determining return intervals for extreme areal precipitation amounts. *Journal of Hydrology*, 315(1-4):203–219.

Anagnostou, E. N. and Krajewski, W. F. (1998). Calibration of the WSR-88D precipitation processing subsystem. *Weather and Forecasting*, 13(2):396–406.

Aniol, R., Riedl, J., and Dieringer, M. (1980). Über kleinräumige und zeitliche Variationen der Niederschlagsintensität. *Meteorol. Rundsch.*, (33):50–56.

Atlas, D. and Ulbrich, C. W. (1977). Path- and area-integrated rainfall measurement by microwave attenuation in the 1-3 cm band. *Journal of Applied Meteorology*, 16(12):1322–1331.

Barnes, S. L. (1964). A technique for maximizing details in numerical weather map analysis. *Journal of Applied Meteorology*, 3(4):396–409.

Bartels, H., Weigl, E., Reich, T., Lang, P., Wagner, A., Kohler, O., and Gerlach, N. (2004). Projekt RADOLAN - Routineverfahren zur online-Aneichung der Radarniederschlagsdaten mit Hilfe von automatischen Bodenniederschlagsstationen (Ombrometer). Technical report, Deutscher Wetterdienst, Offenbach am Main/Germany.

Battan, L. J. (1973). *Radar observation of the atmosphere*. University of Chicago Press, Chicago, rev. ed edition.

Battan, L. J. and Atlas, D., editors (1990). *Radar in meteorology: Battan Memorial and 40th Anniversary Radar Meteorology Conference*. American Meteorological Society, Boston.

Baumgartner, A. (1996). *Allgemeine Hydrologie - quantitative Hydrologie: mit 126 Tabellen*. Borntraeger, Berlin; Stuttgart [u.a.].

Bech, J., Codina, B., Lorente, J., and Bebbington, D. (2003). The sensitivity of single polarization weather radar beam blockage correction to variability in the vertical refractivity gradient. *Journal of Atmospheric and Oceanic Technology*, 20(6):845–855.

Becker, A. (2013). Requirements for weather radar data. In *Workshop on radar data exchange*, Exeter. World Meteorological Organization.

Berndt, C., Rabiei, E., and Haberlandt, U. (2014). Geostatistical merging of rain gauge and radar data for high temporal resolutions and various station density scenarios. *Journal of Hydrology*, 508:88–101.

Bernstein, L., Pachauri, R. K., Reisinger, A., and Intergovernmental Panel on Climate Change (2008). *Climate change 2007: synthesis report*. IPCC, Geneva, Switzerland.

Brandes, E. A. (1975). Optimizing rainfall estimates with the aid of radar. *Journal of Applied Meteorology*, 14(7):1339–1345.

Bringi, V. N. (2001). *Polarimetric Doppler weather radar: principles and applications*. Cambridge University Press, Cambridge ; New York.

Chang, N.-B. (2012). *Multiscale hydrologic remote sensing perspectives and applications*. Taylor & Francis, Boca Raton.

Collier, C. (1986). Accuracy of rainfall estimates by radar, part i: Calibration by telemetering raingauges. *Journal of Hydrology*, 83(3-4):207–223.

Collier, C. G. (1989). *Applications of weather radar systems: a guide to uses of radar data in meteorology and hydrology*. The Ellis Horwood library of space science and space technology. Horwood ; Halsted Press, Chichester : New York.

Davie, T. (2008). *Fundamentals of hydrology*. Routledge, London; New York.

DIN (2008). DIN EN 752 - Entwässerungssysteme auSSerhalb von Gebäuden. DIN, Beuth-Verlag, Berlin.

Doviak, R. J. (2006). *Doppler radar and weather observations*. Dover Publications, Mineola, N.Y, 2nd ed., Dover ed edition.

DWA (2006). Hydraulische Dimensionierung und Leistungsnachweis von Abwasserkanälen und -leitungen. Technical report, Beuth-Verlag, Berlin.

DWD (2009). Beschreibung des Kompositformats Version 2.2.1. Technical report, Deutscher Wetterdienst, Offenbach am Main.

Dyck, S. and Peschke, G. (1995). *Grundlagen der Hydrologie*. Verl. für Bauwesen, Berlin.

Ehret, U., Götzinger, J., Bárdossy, A., and Pegram, G. (2008). Radar-based flood forecasting in small catchments, exemplified by the goldersbach catchment, germany. *International Journal of River Basin Management*, 6(4):323–329.

Eischeid, J. K., Bruce Baker, C., Karl, T. R., and Diaz, H. F. (1995). The quality control of long-term climatological data using objective data analysis. *Journal of Applied Meteorology*, 34(12):2787–2795.

Fornasiero, A., Bech, J., and Alberoni, P. P. (2006). Enhanced radar precipitation estimates using a combined clutter and beam blockage correction technique. *Natural Hazards and Earth System Science*, 6(5):697–710.

García-Pintado, J., Barberá, G. G., Erena, M., and Castillo, V. M. (2009). Rainfall estimation by rain gauge-radar combination: A concurrent multiplicative-additive approach: Multicative-additive rain gauge-radar merging. *Water Resources Research*, 45(1).

Gebremichael, M. and Hossain, F., editors (2010). *Satellite rainfall applications for surface hydrology*. Springer, Dordrecht ; New York.

Giles, J. (2002). Scientific uncertainty: When doubt is a sure thing. *Nature*, 418(6897):476–478.

Goovaerts, P. (1997). *Geostatistics for natural resources evaluation*. Applied geostatistics series. Oxford University Press, New York.

Goudenhoofdt, E. and Delobbe, L. (2009). Evaluation of radar-gauge merging methods for quantitative precipitation estimates. *Hydrology and Earth System Sciences*, 13(2):195–203.

Görner, C., Jatho, N., and Bernhofer, C. (2011). Applicability of satellite-based rainfall algorithms for estimating flood-related rainfall events in the mid-latitudes. part i: spatial integration. *Journal of Flood Risk Management*, 4(3):176–188.

Görner, C., Kronenberg, R., and Bernhofer, C. (2012). Applicability of satellite-based rainfall algorithms for estimating flood-related rainfall events in the mid-latitudes. part II: temporal integration: Satellite-based rainfall algorithms for estimating rainfall events. *Journal of Flood Risk Management*, 5(2):175–186.

Hahmann, S., Burghardt, D., and Weber, B. (2011). 80% of all information is geospatially referenced - towards a research framework: Using the semantic web for (In)Validating this famous geo assertion. pages 1–9, Universiteit Utrecht.

He, X. (2011). *Weather radar based quantitative precipitation estimation in modeling of catchment hydrology*. PhD thesis, University of Copenhagen, Copenhagen/Denmark.

Hengstebeck, T., Helmert, K., and Seltmann, J. (2010). Radarqs - a standard quality control software for radar data at DWD.

Holawe, F. and Dutter, R. (1999). Geostatistical study of precipitation series in austria: time and space. *Journal of Hydrology*, 219(1-2):70–82.

Höppner, F., editor (1999). *Fuzzy cluster analysis: methods for classification, data analysis, and image recognition*. J. Wiley, Chichester ; New York.

Huffman, G. J., Bolvin, D. T., Nelkin, E. J., Wolff, D. B., Adler, R. F., Gu, G., Hong, Y., Bowman, K. P., and Stocker, E. F. (2007). The TRMM multisatellite precipitation analysis (TMPA): quasi-global, multiyear, combined-sensor precipitation estimates at fine scales. *Journal of Hydrometeorology*, 8(1):38–55.

Karamouz, M., Nazif, S., and Falahi, M. (2013). *Hydrology and hydroclimatology: principles and applications*.

Knott, E. F. (2004). *Radar cross section*. SciTech radar and defense series. SciTech Pub, Raleigh, NC, 2nd ed., corr. reprinting edition.

Kraus, H. (2004). *Die Atmosphäre der Erde: eine Einführung in die Meteorologie*. Springer, Berlin [u.a.].

Kraus, H. (2008). *Grundlagen der Grenzschicht-Meteorologie: Einführung in die Physik der atmosphärischen Grenzschicht und in die Mikrometeorologie*. Springer, Berlin; Heidelberg; New York.

Krämer, S. and Verworn, H.-R. (2005). Radar rainfall time series for the performance assessment of sewer systems. In *Proc. 10th Int. Conf. on Urban Drainage*, Copenhagen/Denmark.

Kronenberg, R., Barfus, K., Franke, J., and Bernhofer, C. (2013). On the downscaling of meteorological fields using recurrent networks for modelling the water balance in a meso-scale catchment area of saxony, germany. *Atmospheric and Climate Sciences*, 03(04):552–561.

Lang, P. (1997). Niederschlagsquantifizierung auf der basis von radardaten. In *promet*, volume 1-2 of *26*, pages 22–31. Deutscher Wetterdienst, Offenbach am Main/Germany.

Laws, J. O. and Parsons, D. A. (1943). The relation of raindrop-size to intensity. *Transactions, American Geophysical Union*, 24(2):452.

Levizzani, V., Bauer, P., and Turk, F. J., editors (2007). *Measuring precipitation from space: EURAINSAT and the future*. Number v. 28 in Advances in global change research. Springer, Dordrecht, The Netherlands.

Maniak, U. (2010). *Hydrologie und Wasserwirtschaft Eine Einführung für Ingenieure*. Springer-Verlag Berlin Heidelberg, Berlin, Heidelberg.

Marshall, J. S. and Palmer, W. M. K. (1948). The distribution of raindrops with size. *Journal of Meteorology*, 5(4):165–166.

Marx, A. (2007). *Einsatz gekoppelter Modelle und Wetterradar zur Abschätzung von Niederschlagsintensitäten und zur Abflussvorhersage*. PhD thesis, Inst. für Wasser- und Umweltsystemmodellierung, Stuttgart.

Meetschen, D. and Simmer, C. (2005). Warnung vor starkniederschlägen mittels niederschlagsradar. In *Entscheidungsunterstützung in der Wasserwirtschaft - Von der Theorie zum Anwendungsfall*, Beiträge zum Tag der Hydrologie 2005, 22./23. März, 2005, Aachen, Forum für Hydrologie und Wasserbewirtschaftung, Heft 10.05, pages 209–216. Aachen.

Michaelides, S., editor (2008). *Precipitation: advances in measurement, estimation, and prediction*. Springer, Berlin.

Michelson, D. and Koistinen, J. (2000). Gauge-radar network adjustment for the baltic sea experiment. *Physics and Chemistry of the Earth, Part B: Hydrology, Oceans and Atmosphere*, 25(10-12):915–920.

Mittermaier, M. P., Hogan, R. J., and Illingworth, A. J. (2004). Using mesoscale model winds for correcting wind-drift errors in radar estimates of surface rainfall. *Quarterly Journal of the Royal Meteorological Society*, 130(601):2105–2123.

Oke, T. R. (1992). *Boundary layer climates*. Routledge, London; New York.

Overeem, A. (2009). *Climatology of extreme rainfall from rain gauges and weather radar*. PhD thesis, Wageningen University, Wageningen, NL.

Overeem, A., Buishand, T. A., and Holleman, I. (2009). Extreme rainfall analysis and estimation of depth-duration-frequency curves using weather radar: Rainfall analysis, estimation of ddf curves. *Water Resources Research*, 45(10).

Overeem, A., Buishand, T. A., Holleman, I., and Uijlenhoet, R. (2010). Extreme value modeling of areal rainfall from weather radar: Extreme value modelling of areal rainfall. *Water Resources Research*, 46(9).

Palmer, R. (2010). *World Environmental and Water Resources Congress 2010 Challenges of Change*. American Society of Civil Engineers, Reston.

Pearson, K. (1901). On lines and planes of closest fit to systems of points in space. *Philosophical Magazine Series 6*, 2(11):559–572.

Pfaff, T. (2013). *Processing and analysis of weather radar data for use in hydrology*. PhD thesis, Inst. für Wasser- und Umweltsystemmodellierung, Stuttgart.

Probert-Jones, J. R. (1962). The radar equation in meteorology. *Quarterly Journal of the Royal Meteorological Society*, 88(378):485–495.

Raghavan, S. (2003). *Radar meteorology*. Number v. 27 in Atmospheric and oceanographic sciences library. Kluwer Academic Publishers, Dordrecht ; Boston.

Rauthe, M., Steiner, H., Riediger, U., Mazurkiewicz, A., and Gratzki, A. (2013). A central european precipitation climatology - part i: Generation and validation of a high-resolution gridded daily data set (HYRAS). *Meteorologische Zeitschrift*, 22(3):235–256.

Richter, D. (1995). *Ergebnisse methodischer Untersuchungen zur Korrektur des systematischen Meßfehlers des Hellmann-Niederschlagsmessers*. Selbstverl. des Dt. Wetterdienstes, Offenbach am Main.

Riedl, J. (1986). RADAR - Flächenniederschlagsmessung. In *promet*, number 2-3, pages 20–23. Deutscher Wetterdienst, Offenbach am Main/Germany.

Rinehart, R. E. (2004). *Radar for meteorologists, or, You too can be a radar meteorologist, part III*. Rinehart Publications, Columbia, MO.

Schönwiese, C.-D. (2013). *Klimatologie*. Ulmer, Stuttgart.

Sevruk, B. (1974). Evaporation losses from containers of Hellmann precipitation gauges. *Hydrological Sciences Bulletin*, 19(2):231–236.

Sevruk, B. (1982). Method of correction for systematic error in point precipitation measurement for operational use. Operational Hydrological Report 21, World Meteorological Organisation, Genf, Switzerland.

Smalley, M., L'Ecuyer, T., Lebsock, M., and Haynes, J. (2014). A comparison of precipitation occurrence from the NCEP stage IV QPE product and the *CloudSat* cloud profiling radar. *Journal of Hydrometeorology*, 15(1):444–458.

Steiner, M., Smith, J. A., Burges, S. J., Alonso, C. V., and Darden, R. W. (1999). Effect of bias adjustment and rain gauge data quality control on radar rainfall estimation. *Water Resources Research*, 35(8):2487–2503.

Stephens, G. L. (1994). *Remote sensing of the lower atmosphere: an introduction*. Oxford University Press, New York.

Stephens, G. L., Vane, D. G., Boain, R. J., Mace, G. G., Sassen, K., Wang, Z., Illingworth, A. J., O'Connor, E. J., Rossow, W. B., Durden, S. L., Miller, S. D., Austin, R. T., Benedetti, A., Mitrescu, C., and CloudSat Science Team, T. (2002). The cloudsat mission and the a-train: A new dimension of space-based observations of clouds and precipitation. *Bulletin of the American Meteorological Society*, 83(12):1771–1790.

Storch, H. v. (2001). *Statistical analysis in climate research*. Cambridge University Press, Cambridge, UK ; New York, 1st pbk. ed. (with corrections) edition.

Straka, J. M. (2009). *Cloud and precipitation microphysics principles and parameterizations*. Cambridge University Press, Cambridge, UK; New York.

Strangeways, I. (2007). *Precipitation: theory, measurement and distribution*. Cambridge University Press, Cambridge ; New York.

Sumner, G. (1996). Daily precipitation patterns over wales: Towards a detailed precipitation climatology. *Transactions of the Institute of British Geographers*, 21(1):157.

Sumner, G. N. (1988). *Precipitation: process and analysis*. Wiley, Chichester West Sussex ; New York.

Sun, S. and Bertrand-Krajewski, J.-L. (2013). Separately accounting for uncertainties in rainfall and runoff: Calibration of event-based conceptual hydrological models in small urban catchments using bayesian method: Separate uncertainties in rainfall and runoff in calibration. *Water Resources Research*, 49(9):5381–5394.

Thies, B. and Bendix, J. (2011). Satellite based remote sensing of weather and climate: recent achievements and future perspectives. *Meteorological Applications*, 18(3):262–295.

Toth, M., Jones, E., Pittman, D., and Solomon, D. (2011). DOW radar observations of wind farms. *Bulletin of the American Meteorological Society*, 92(8):987–995.

van de Beek, C. Z., Leijnse, H., Torfs, P. J. J. F., and Uijlenhoet, R. (2011). Climatology of daily rainfall semi-variance in the netherlands. *Hydrology and Earth System Sciences*, 15(1):171–183.

Velasco-Forero, C. A., Sempere-Torres, D., Cassiraga, E. F., and Jaime Gómez-Hernández, J. (2009). A non-parametric automatic blending methodology to estimate rainfall fields from rain gauge and radar data. *Advances in Water Resources*, 32(7):986–1002.

Verworn, A. and Haberlandt, U. (2011). Spatial interpolation of hourly rainfall-effect of additional information, variogram inference and storm properties. *Hydrology and Earth System Sciences*, 15(2):569–584.

von Hardenberg, J., Ferraris, L., Rebora, N., and Provenzale, A. (2007). Meteorological uncertainty and rainfall downscaling. *Nonlinear Processes in Geophysics*, 14(3):193–199.

Wackernagel, H. (2003). *Multivariate geostatistics: an introduction with applications*. Springer, Berlin; New York.

Walther, A. (2007). *Radar-based precipitation classification in the Baltic Sea area*. PhD thesis, Freien Universität Berlin, Berlin.

Webb, T. L. (2013). Are we entering a new golden age of radar meteorology in the UK? *Weather*, 68(8):222–222.

Weigl, E. and Winterrath, T. (2009). Radargestützte niederschlagsanalyse und -vorhersage (RADOLAN, RADVOR-OP). In *promet*, volume 1-3 of *35*, pages 78–86. Deutscher Wetterdienst, Offenbach am Main/Germany, 3450 edition.

Wilks, D. S. (2011). *Statistical methods in the atmospheric sciences*. Academic Press, Oxford; Waltham, MA.

Wilson, J. W. and Brandes, E. A. (1979). Radar measurement of rainfall - summary. *Bulletin of the American Meteorological Society*, 60(9):1048–1058.

World Meteorological Organization (2008). *Guide to hydrological practices*. Number no. 168 in WMO. WMO, Geneva, Switzerland, 6th ed edition.

LIST OF FIGURES

LIST OF TABLES

LIST OF ABBREVIATIONS

Abbreviation	Description
BRA	Brandes Spatial Adjustment
DWD	German Weather Service
EDK	External Drift Kriging
MFBC	Mean Field Bias Correction
QPE	Quantitative Precipitation Estimates
RDA	Range-Dependent Adjustment
SRD	Static local bias correction and range dependent adjustment
TRMM	Tropical Rainfall Measuring Mission

LIST OF SYMBOLS

Symbol	Unit	Description
A	$[m^2]$	Sphere surface area
A_g	$[m^2]$	Geometric antennae area
A_W	$[m^2]$	Effective antennae area
B_{BRA}	$[-]$	BRA bias
B_{MFBC}	$[-]$	MFBC bias
B_{RDA}	$[-]$	RDA bias
B_{SLB}	$[-]$	SLB bias
B_{SLC}	$[-]$	SLC bias
C	$[-]$	Radar constant
D	$[mm]$	Droplet diameter
E_t	$[mm]$	Evapotranspiration
G	$[-]$	Antenna gain
K	$[\frac{dB}{km}]$	Material dependent factor
K_a	$[-]$	Efficiency
M	$[\frac{mm^6}{m^3}]$	Integral reflectivity
N	$[-]$	Number of precipitation / cloud particles
P	$[mm]$	Precipitation
P_E	$[W]$	Power at the receiver
P_e	$[W]$	Power at the receiver
P_r	$[W]$	Reflected power
P_S	$[W]$	Transmitted power
Q	$[mm]$	Discharge
R	$[\frac{mm}{h}]$	Rain rate
$\Re$	$[mm]$	Radar-derived rain rate
S	$[mm]$	Station value
S_e	$[\frac{W}{m^2}]$	Power density at the receiver
S_g	$[\frac{W}{m^2}]$	Directional power density
S_u	$[\frac{W}{m^2}]$	Non-directional power density
ΔS	$[mm]$	Storage term
V	$[m^3]$	Impulse volume
Z	$[\frac{mm^6}{m^3}]$	Reflectivity

a	$[-]$	Coefficient of Z-R relation
b	$[-]$	Coefficient of Z-R relation
c_0	$[\frac{m}{s}]$	Speed of light
d	$[m]$	Distance
h	$[m]$	Separation distance
l	$[-]$	Coefficient of polynomial
n	$[-]$	Number of stations
p	$[-]$	Coefficient of polynomial
o	$[-]$	Coefficient of polynomial
r	$[m]$	Distance antenna-target-antenna
r_c	$[m]$	Sphere radius
r_{RDA}	$[m]$	Sphere radius
r_V	$[m]$	Radius of impulse volume
r_1	$[m]$	Distance antenna-target
r_2	$[m]$	Distance target-antenna
u	$[-]$	Smoothing factor
w	$[-]$	Weighting factor
x	$[-]$	Moment
Γ	$[-]$	Gamma function
Λ	$[-]$	Empirical parameter
ϵ	$[-]$	Permittivity
θ	$[\circ]$	Elevation angle
λ	$[m]$	Transmitters wavelength
π	$[-]$	Ratio of a circle's circumference to its diameter
σ	$[m^2]$	Scattering cross section
$\sum_{vol} \sigma$	$[-]$	Back scattering cross section per unite volume
τ	$[s]$	Travel time
ϕ	$[\circ]$	Vertical beam width of antennas pattern

LIST OF THE AUTHOR'S PUBLICATIONS

Peer-reviewed Publications

(1) Görner, C., Kronenberg, R. and Bernhofer, C. (2012). Applicability of satellite-based rainfall algorithms for estimating flood-related rainfall events in the mid-latitudes. Part II: temporal integration, Journal of Flood Risk Management, DOI: 10.1111/j.1753-318X.2012.01138.x.

(2) Kronenberg, R., Franke, J. and Bernhofer, C. (2012). Classification of daily precipitation patterns on the basis of radar derived precipitation rates for Saxony, Germany, Meteorologische Zeitschrift, Vol. 21, No. 5, 475-486.

(3) Kronenberg, R., Franke, J. and Bernhofer, C. (2013). Comparison of different approaches to fit log-normal mixtures on radar-derived precipitation data, Meteorological Applications, Vol. 21, No. 3, 743-754.

(4) Kronenberg, R., Barfus, K., Franke, J. and Bernhofer, C. (2013). On the downscaling of meteorological fields using recurrent networks for modelling the water balance in a meso-scale catchment area of Saxony, Germany, Atmospheric and Climate Sciences, Vol. 3, No. 4, 552-561.

(5) Kronenberg, R., Güttler, T., Franke, J. and Bernhofer, C. (2013). Application of synthetic meteorological time series in BROOK90: A case study for the Tharandt Forest, Germany, Open Journal of Modern Hydrology, Vol. 3, No. 4, 214-225.

(6) Kronenberg, R. and Bernhofer, C. (2014). A methode to adapt radar-derived precipitation fields for climatological applications, Meteorological Applications, DOI:10.1002/met.met.1498.

Conferences and Workshops

(1) Kronenberg R. (2012). Klassifikation von täglichen Niederschlagsmustern auf Grundlage von RADOLAN-Daten für die erweiterte REGKLAM - Modellregion, Fachausschuss Hydrometeorologie der Deutschen Meteorologischen Gesellschaft, Offenbach am Main.

(2) Kronenberg R., Franke J. and Bernhofer C. (2012). Spatial scale-dependent comparison of different approaches to fit mixture distributions on radar-derived precipitation data, UrbanRain2012, St. Moritz.

(3) Kronenberg R. (2013). Assessing field significance of kolmogorov-smirnov tests on spatially correlated precipitation data, Lomonossow Conference, Moscow.

(4) Kronenberg R., Franke J. and Bernhofer C. (2013). Detection of potential transition areas of changing climatic conditions at a regional scale until 2100 for Saxony, Germany, DACH2013, Innsbruck.

DANKSAGUNG

Hiermit möchte ich mich recht herzlich bei Herrn Prof. Dr. Christian Bernhofer bedanken, der mir über eine Anstellung als wissenschaftlicher Mitarbeiter an seiner Professur die Möglichkeit zur Erstellung dieser Arbeit gegeben hat. Hervorheben möchte ich hier seine vielseitige Unterstützung und das mir entgegengebrachte Vertrauen und die damit verbundene Freizügigkeit bei der Themengestaltung dieser Arbeit.

Weiterer Dank gilt Herrn Prof. Dr. Clemens Simmer und Herrn Prof. Dr. Lars Bernard für das Anfertigen ihrer Gutachten zu dieser Arbeit.

Die Dissertation wurde gefördert durch das Bundesministerium für Bildung und Forschung (BMBF) im Rahmen des Projektes REGKLAM (Förderkennzeichen: 01LR0802B), durch den Deutschen Akademischen Austauschdienst (DAAD) und dem Erasmus Mundus Action 2 Programm der Europäischen Union. Auch hierfür gilt mein Dank.

Ebenso gilt mein Dank Dr. Johannes Franke, Dr. Klemens Barfus und den Mitarbeitern der Professur für Meteorologie an der TU Dresden für die fruchtbaren Diskussionen und zahlreichen Denkanstöse.

Prof. Dr. Alexander Krishenko und Dr. Yana Kinderknecht, sowie den Mitarbeitern vom Lehrstuhl für Mathematische Modellierung an der Bauman Moskauer Staatlichen Technischen Universität danke ich für die herzliche Betreuung und das angenehme Arbeitsklima.

Ich danke meinen Eltern, meinen Brüdern und meiner Familie für die Unterstützung, das Verständnis und für die zahlreichen schönen Erinnerungen die mich immer begleiten werden.

Ich danke Torsten-Michael Frenzel für, nun dafür, dass ich mehr als die Hälfte gesehen habe und natürlich möchte ich mich bei meiner Frau Yulia bedanken: Cpasibo tebe za tebya!

ERKLÄRUNG

Hiermit erkläre ich, Rico Sascha Kronenberg, die vorliegende Arbeit selbstständig und ohne die Hilfe anderer Personen angefertigt zu haben. Weiterhin versichere ich, nur frei zugängliche oder lizenzierte Software verwendet zu haben, welche mir im Rahmen einer Anstellung als wissenschaftlicher Mitarbeiter an der Professur für Meteorologie des Institutes für Hydrologie und Meteorologie der Technischen Universität Dresden zur Verfügung stand.

Ich bestätige, dass ich die Promotionsordnung der Fakultät Umweltwissenschaften der TU Dresden anerkenne.

Dresden, 15. Oktober 2014

Figure 4.1: David and Goliath, by R. Kronenberg after an academic drawing by D.Shelinsky (1948)